HHS Public Access

Author manuscript

Sci Immunol. Author manuscript; available in PMC 2022 August 25.

Published in final edited form as:

Sci Immunol. 2022 July 22; 7(73): eabl4102. doi:10.1126/sciimmunol.abl4102.

A clade C HIV-1 vaccine protects against heterologous SHIV infection by modulating IgG glycosylation and T helper response in macaques

Anusmita Sahoo[1,2], **Andrew T Jones**[1,2], **Narayanaiah Cheedarla**[1,2], **Sailaja Gangadhara**[1,2], **Vicky Roy**[3], **Tiffany M Styles**[1,2], **Ayalnesh Shiferaw**[1,2], **Korey L Walter**[4], **LaTonya D Williams**[5], **Xiaoying Shen**[5], **Gabriel Ozorowski**[6], **Wen-Hsin Lee**[6], **Samantha Burton**[1,7], **Lasanajak Yi**[8], **Xuezheng Song**[8], **Zhaohui Qin**[9], **Cynthia A Derdeyn**[1,7], **Andrew B Ward**[6], **John D Clements**[10], **Raghavan Varadarajan**[11,12], **Georgia D Tomaras**[5], **Pamela A Kozlowski**[4], **Galit Alter**[3], **Rama Rao Amara**[1,2,13,*]

[1]Emory Vaccine Center, Yerkes National Primate Research Center, Emory University, Atlanta, Georgia 30329, USA

[2]Department of Microbiology and Immunology, Emory School of Medicine, Emory University, Atlanta, Georgia 30322, USA

[3]Ragon Institute of MGH, MIT, and Harvard, Cambridge, MA 02139, USA

[4]Department of Microbiology, Immunology and Parasitology, Louisiana State University Health Sciences Center, New Orleans, Louisiana 70112, USA

[5]Department of Surgery, Duke University Medical School, Duke University, Durham, North Carolina 27710, USA

[6]Department of Integrative Structural and Computational Biology, The Scripps Research Institute, San Diego, California 92121, USA

[7]Department of Pathology and Laboratory Medicine, School of Medicine, Emory University, Atlanta, GA, 30322, USA

[8]Department of Biochemistry, Emory Glycomics and Molecular Interactions Core (EGMIC), School of Medicine, Emory University, Atlanta, GA, 30322, USA

[*]Correspondence should be addressed to Dr. Rama R Amara. Phone: (404) 727-8765; FAX: (404) 727-7768; ramara@emory.edu.

Author Contributions

R.R.A., A.Sahoo, A.T.J. designed the study. R.R.A. and A.Sahoo wrote the manuscript. R.R.A, A.Sahoo, A.T.J, T.M.S, V.R, S.B, C.D, R.V, G.D.T, P.A.K, J.D.C, provided edits to the manuscript. A.Sahoo, A.T.J., N.C., performed experiments and analyzed data. A.Sahoo designed C.1086 CycP gp120, Conc-C CycP gp120, purified the protein constructs described in the study, performed Fc glycoform related experiments and analyses for pre-vaccination samples (supervised by X.Song and L.Y), S.G constructed and prepared rMVAs, T.M.S did ADCC, V.R. (supervised by G.A) did serum isotyping, ADNP, ADCP and Fc glycoform analyses for serum collected after protein boost, K.L.W. (supervised by P.A.K) performed mucosal antibody measurements and ADCVI assay, X.Shen and L.D.W. designed and analyzed the BAMA assay (supervised by G.D.T.), G.O and W-H.L. did NS-EM (supervised by A.W.), S.B. (supervised by C.D.) performed the neutralization assays, R.V. contributed to design of 16055 CycP gp120, J.D.C. provided dmLT, Q.Z. calculated vaccine efficacy and helped with statistical analyses, A.Shiferaw performed experiments.

Competing interests

R.R.A, A.J and R.V are co-inventors of MVA/CycP-gp120 vaccine technology. Emory university filed a patent on this technology. Other authors declare no competing interests.

Data and materials availability

All unique plasmids generated in this study may be requested from the authors with a completed Materials Transfer Agreement. All data needed to evaluate the conclusions in the paper are present in the paper or the Supplementary Materials

[9]Department of Biostatistics and Bioinformatics, Rollins School of Public Health, Emory University, Atlanta, GA, 30322, USA

[10]Department of Microbiology and Immunology, Tulane University School of Medicine, New Orleans, LA, 8638, USA

[11]Molecular Biophysics Unit (MBU), Indian Institute of Science, Bengaluru, Karnataka 560012, India

[12]Jawaharlal Nehru Centre for Advanced Scientific Research, Jakkur, Bengaluru, Karnataka 560012, India

[13]Lead Contact

Abstract

The rising global HIV-1 burden urgently requires vaccines capable of providing heterologous protection. Here, we developed a clade C HIV-1 vaccine consisting of priming with modified vaccinia Ankara (MVA) and boosting with cyclically permuted trimeric gp120 (CycP-gp120) protein, delivered either orally using a needle-free injector or through parenteral injection. We tested protective efficacy of the vaccine against intrarectal challenges with a pathogenic heterologous clade C SHIV infection in rhesus macaques. Both routes of vaccination induced a strong envelope-specific IgG in serum and rectal secretions directed against V1V2 scaffolds from a global panel of viruses with polyfunctional activities. Envelope-specific IgG showed lower fucosylation compared to total IgG at baseline, and most of the vaccine-induced proliferating blood $CD4^+$ T cells did not express CCR5 and $\alpha4\beta7$, markers associated with HIV target cells. Following SHIV challenge, both routes of vaccination conferred significant and equivalent protection, with 40% of animals remaining uninfected at the end of six weekly repeated challenges with an estimated efficacy of 68% per exposure. Induction of envelope-specific IgG correlated positively with G1FB glycosylation, and G2S2F glycosylation correlated negatively with protection. Vaccine-induced $TNF\alpha^+IFN\gamma^+$ $CD8^+$ T cells and $TNF\alpha^+$ $CD4^+$ T cells expressing low levels of CCR5 in the rectum at pre-challenge were associated with decreased risk of SHIV acquisition. These results demonstrate that the clade C MVA/CycP-gp120 vaccine provides heterologous protection against a tier2 SHIV rectal challenge by inducing a polyfunctional antibody response with distinct Fc glycosylation profile, as well as cytotoxic CD8 T cell response and CCR5 negative T helper response in the rectum.

One sentence summary

The glycosylation profile of IgG and HIV resistant T helper response induced by vaccination contribute to HIV vaccine protection

Introduction

Currently there are nearly 38 million people infected with HIV-1 and there is a great need for the development of effective vaccines to prevent HIV-1 infection. Broadly neutralizing antibodies (bnAbs) are essential for the prevention of HIV-1 infection. However, given the very high inter and intra clade diversity of HIV-1, the vaccines should generate a broadly

cross-reactive neutralizing antibody response which has been a far-reaching goal. Immune correlate analyses from the RV144 clinical trial, the only HIV-1 vaccine efficacy trial to date to show some efficacy to date, identified that IgG antibodies against Murine Leukemia Virus gp70 scaffolded V1V2 (gp70-V1V2) region of HIV-1 envelope (Env) correlated with reduced infection risk (1–4). In addition, multiple vaccine efficacy studies in non-human primates (NHPs) have highlighted the importance of gp70-V1V2 specific antibodies and "polyfunctional" non-neutralizing antibodies (non-nAbs) with effector functions in mediating protective immunity (5, 6).

The Fc mediated functional activity of an antibody is critically regulated by its ability to bind to Fc receptors on different effector cells. Accordingly, the IgG subclass of the antibody regulates various effector functions, and the IgG subclass of vaccine-induced antibody response can be influenced by the vaccination modality (7). For example, the ALVAC prime/gp120 protein boost approach used in the RV144 trial has been shown to induce greater IgG3 response compared to gp120-only immunizations used in the VaxGen trial, and the lack of efficacy in the latter was partly attributed to lower induction of IgG3 responses (8). In addition to IgG subclass, the effector functions of the antibody are shaped by the glycan composition of the antibody in its Fc region (9, 10). Studies have demonstrated that variations in Fc glycosylation of HIV Env-specific antibodies are associated with time to viral rebound following analytical treatment interruption (11), and can differentiate neutralizers from non-neutralizers (12), spontaneous control of viral replication in HIV controllers, and improve antiviral activity (10). In addition to the antibody response, strong induction of virus-specific $CD8^+$ T cells, in particular tissue-resident memory $CD8^+$ T cells, have been shown to contribute for better protection (13), while strong induction of Th1-biased $CD4^+$ T cells has been shown to contribute towards diminished protection (14). Thus, the effectiveness of an HIV-1 vaccine depends on its ability to elicit multidimensional balanced immune responses.

Mucosal tissues are the major ports for viral entry in HIV-1 infection and the gut serves as a major site for HIV/SIV viral replication (15). Hence, an effective vaccine should be able to deliver protective control of infection at mucosal sites by establishing resident memory T cells and functional antibody responses at these sites. In general, mucosal vaccinations induce much stronger mucosal immunity compared to parenteral vaccinations. Several studies (reviewed in (16)) have shown the leverage of mucosal immunization over parenteral vaccination to reduce viremia in mucosal simian-human immunodeficiency virus (SHIV) challenge NHP models. For example, intrarectal but not parenteral vaccination with peptides specific to HIV-1 Env helper epitope and SIV gag or pol CTL epitope reduced viremia after intrarectal challenge with a pathogenic SHIV (17). Similarly, intranasal but not intravenous administration of non-pathogenic SHIV infection generated protection against intravaginal SHIV-89.6P challenge (18). Thus, mucosal vaccination approaches have the ability to provide significant protection against HIV-1.

Heterologous prime/boost vaccination regimens are popular due to their ability to induce a strong and broad humoral and cellular immunity. Towards this, we developed a HIV-1 vaccination regimen consisting of priming with modified vaccinia Ankara (MVA) and boosting with a cyclically permuted trimeric gp120 protein (MVA/CycP-gp120). The

MVA-HIV platform has been extensively characterized and tested in clinical studies as potential vaccine candidate for HIV-1 (19–21). We previously described the design of cyclically permuted (CycP) derivative of clade B gp120s which efficiently formed stable homogeneous trimers, displayed enhanced binding to multiple bnAbs compared to their gp120 counterparts and elicited broadly cross-reactive V1V2 scaffold specific antibodies in rabbits and in rhesus macaques (22–24). In a recent pilot study, we compared the immunogenicity and efficacy of MVA/CycP-gp120 clade B vaccine approach delivered via either oral route using needle-free (NF) injector or topical application or parenteral route (intradermal for MVA and subcutaneous for protein - ID/SC) (25). The protein boosts were adjuvanted with double-mutant heat-labile enterotoxin LT (R192G/L211A) from *Escherichia coli* (dmLT) (26, 27) as a mucosal adjuvant. Oral immunization resulted in induction of stronger Env-specific antibody responses in both systemic and mucosal compartments and higher vaginal IgA which was otherwise below the detection limit in the systemic route. Both oral (NF-Oral) and parenteral (intradermal/subcutaneous ID/SC) immunization routes significantly delayed acquisition of mucosal SHIV infection compared to the unvaccinated controls and highlighted the potential of this vaccination regimen to provide protection against HIV-1.

In our NF-Oral study we used a significantly higher dose of dmLT adjuvant for oral immunization (50μg/dose) compared to ID/SC immunization (2μg/dose). In addition, we used the needle-free injector device Syrijet that was developed for use by dentists and not ideal for human immunizations. The current study was designed using a fixed (5μg) amount of adjuvant for both oral and parenteral immunization routes to evaluate whether (a) the protective efficacy of MVA/CycP-gp120 design could be generalized and extended to clade C immunogens in order to offer protection against clade C HIV-1 infections, that represent the majority in the world, (b) a lower dose of dmLT adjuvant administered orally can induce protective immunity in systemic and mucosal compartments, (c) PharmaJet, a needle-free immunization device that was developed for parenteral immunizations, can be used for oral immunizations, and (d) to identify immune correlates of protection for both routes of immunization. Our results demonstrated that both routes of immunization induce strong and comparable titers of Env-specific antibody response in serum and mucosal secretions with polyfunctional activity and provide significant protection from infection and control virus replication. We also demonstrate that vaccination routes differentially influence proliferation of Th17 ($CXCR3^{-}CCR6^{+}$) polarized $CD4^{+}$ T cells. In addition, we showed that the Fc glycosylation profile of vaccine-induced antibody response is distinct from that of baseline total IgG and revealed important associations between Fc glycosylation, antibody effector function and vaccine mediated protection.

Results

Conc-C CycP gp120 efficiently forms trimers and presents a “native-like” epitope recognized by V2 directed bnAbs

Here, we designed clade C based consensus C (Conc-C), C.1086 and 16055 versions of CycP proteins (Fig. 1A and fig. S1A) and compared their biophysical properties. Briefly, the native N and C termini of gp120 protein were connected by a 20 amino acid linker

and a new N and C termini were created at positions 145 and 144 in the V1 loop region. The length of V1 loop was shorter in C.1086 compared to 16055 and Conc-C, so we matched the length in the former sequences by inserting additional amino acids from the 16055 sequence (as shown in fig. S1, A and B). The coiled-coil trimerization domain of the human cartilage matrix protein (hCMP) was inserted in-frame at position 145 of gp120 to increase trimerization of the protein. The proteins were expressed in 293F cells, and purified using *Galanthus nivalis lectin* (GNL) mediated affinity chromatography followed by isolation of trimers by size-exclusion chromatography (SEC) with high protein yield (mean 18mg/L, fig. S1C). The yield was ~6 times higher than the net trimeric yield that was obtained expressing Clade C gp140 stabilized trimers (C.1086 UFO-v2-RQY^{173} (28) and 16055 NFL (29)). Based on the SEC profiles (Fig. 1B), all three CycP gp120 derivatives efficiently formed trimers (74–81%), which was ~30% higher than their gp120 parents. All CycP gp120 derivatives formed stable trimers, in contrast to their gp120 parents which were unstable and dissociated into trimers, monomers and dimers on native gel (Fig. 1C). The negative stain electron microscopy (EM) analyses supported the presence of trimeric forms of the protein (Fig. 1D), as also implied by SEC traces and BN-PAGE (Fig. 1, B and C).

To select between the CycP-gp120 trimer variants, we compared their antigenic properties by Bio-Layer Interferometry (BLI) using multiple Env-specific bnAbs and non-nAbs. Specifically, we tested bnAbs (V1V2 trimer specific PGT145, PG9, PG16, CD4 binding site (bs) specific HJ16, V3 glycan specific PGT121), and non-nAbs (CD4bs F105, V3 specific 447–52D, 39F). It should be noted that none of the constructs bore any additional changes to enhance binding to bnAbs or reduce affinity towards non-nAbs. All variants had N156 and N160 potential N-glycosylation sites (PNGS), critical for binding of many V2 specific bnAbs (30). Conc-C and 16055 CycPs showed high binding affinity towards PGT145, in contrast to C.1086 CycP trimer and the parent gp120s (Fig. 1, E and F, fig S2A, table S1) which either displayed very weak or no measurable binding. This suggested that insertion of the trimerization domain in the V1 region of Conc-C and 16055 CycPs did not significantly affect the native-like quaternary contacts seen by PGT145 at the V1V2 region. The parent gp120s tested here displayed weak binding to V2 specific PG9 bnAb in contrast to their CycP variants which displayed no measurable binding (fig. S2A) indicating modifications in the CycP designs likely affected the display of this targeted epitope. None of the constructs displayed any measurable binding to PG16. The Conc-C constructs carried PGT121 family dependent N332 PNGS, while C.1086 carried N334 PNGS (31). Amongst the CycP trimers tested, only Conc-C CycP displayed high binding affinity towards V3 glycan specific PGT121 (K_D 1.3nM, Fig. 1, E and F, table S1). Reduced binding of the C.1086 CycP construct (fig. S2A) towards PGT121 compared to its parent gp120 suggested loss of display of V3 targeted epitope on C.1086 CycP due to insertion of hCMP in the V2 region. The 16055 sequence lacked N332 and N334 PNGS and thus showed either weak or no observable binding to PGT121 (Fig. 1E and fig. S2A). The three CycP proteins displayed either similar or higher affinity towards CD4bs bnAb HJ16 than their parent gp120s; Conc-C CycP specifically with undetectable dissociation. All constructs showed high binding affinity towards V3 specific 447–52D, 39F non-nAbs (fig. S2B, table S1). Additionally, we observed higher binding of CycP designs to F105 non-nAb relative to their parent gp120s, likely due to conformational rearrangements to accommodate the insertion

of hCMP trimerization domain at the V1V2 region (Fig. 1E, fig. S2B, table S1). Overall, the SEC, EM and antigenicity data confirmed that Conc-C CycP gp120 efficiently folded into trimers, and a sub-population of the trimer was capable of presenting “native-like” quaternary epitope targeted by the antibodies tested. Thus, we selected Conc-C CycP gp120 trimer as the protein component of the vaccine regimen.

Clade C MVA/CycP-gp120 vaccination induces a strong antibody response in serum and rectal secretions, as well as broad Env and gp70-V1V2 scaffold specific serum responses

To evaluate the immunogenicity and efficacy of Conc-C CycP protein as an HIV-1 vaccine candidate and to compare the parenteral immunizations (ID/SC, n=10) with oral NF delivery (NF-Oral, n=10) we conducted a rhesus macaque study in which we primed animals with the MVA/C.1086-VLP vaccine (1×10^8 pfu/dose) at weeks 0 and 10, then boosted with Conc-C CycP (100μg/dose) at week 22 (Fig. 2A). The MVA vaccine was engineered to express C.1086 Env gp150 and SIVmac239 Gag/Pol (fig. S2C), which forms virus-like particles (VLPs). The ID/SC group received MVA via ID route and protein via SC route. The NF-Oral group received both vaccines in the mouth with the total dose split between buccal and sublingual sites. The protein immunizations were adjuvanted with dmLT (5μg/dose) to promote the generation of mucosal antibody responses. A group of unvaccinated animals (n=10) served as the unvaccinated control group. All animals were challenged weekly intrarectally with SHIV1157ipD3N4 beginning at week 38 for a maximum of 6 challenges (two exposures more than the number required to infect 100% of the unvaccinated controls) or until measured for two consecutive positive viral loads (RNA copies/ml >60).

The MVA prime/protein boost vaccination induced a strong IgG binding antibody response in serum that was comparable between the two groups except after the 1st MVA vaccination at which the ID/SC group showed higher levels than the NF-Oral group (Fig. 2B). The 1st MVA vaccination induced low titers of binding antibodies (geometric mean of 1,301 in ID/SC and 418 in NF-Oral) but the 2nd MVA immunization boosted these titers by 10-fold in the ID/SC group and 33-fold in the NF-Oral group leading to a similar geometric mean titer of about 13,485 in both groups (geometric mean end-point titer of 13,066 in ID/SC, and 13,916 in NF-Oral). These responses contracted by ~10-fold over 10 weeks. The protein immunization boosted these responses strongly in both groups to a titer of about 26,345 (geometric mean considering both groups) which contracted by ~6-fold over 10 weeks by the time of challenge. It was interesting to note that the persistence of antibody response after the 2nd MVA (10-fold contraction) was lower than the persistence observed after the protein boost (5-fold contraction) within the same time frame after vaccination. Binding antibody responses measured against Conc-C CycP gp120 trimer in serum were similar to those observed against C.1086 trimer for both immunization groups (fig. S3A).

The MVA prime/protein boost vaccination also induced a strong C.1086 trimer specific IgG binding antibody response in rectal secretions (Fig. 2C) but a lower response in saliva (Fig. 2D). The responses were comparable between the two groups (Fig. 2, C and D). The expansion and contraction of the mucosal antibody response largely mirrored the serum with peak antibody titers reaching about 4.4 and 2.9 ng/μg of the total IgG (geomean) after the protein boost in rectal and salivary secretions, respectively. These responses subsequently

declined by ~7 and 12-fold in rectal and salivary secretions respectively by the pre-challenge time point. Similar levels of IgG binding antibodies were also observed against the Conc-C CycP gp120 trimer in these mucosal secretions (fig. S3B). Neither immunization routes induced detectable levels of antigen specific IgA in secretions (fig. S3C).

Ig subclass analysis of sera from immunized animals revealed that IgG1 was the dominant subclass with low titers of IgG2 and IgG3 antibodies (Fig. 2E). There was no difference in the induction of any specific IgG subclass between the two immunization regimens. All IgG subclasses and IgA exhibited broad reactivity to env proteins from multiple clades (Fig. 2F and fig. S3D). Immune correlates in the RV144 clinical trial and multiple SIV and SHIV challenge studies in rhesus macaques have shown a positive association between V1V2-scaffold specific antibodies and reduced risk of infection (2, 5, 32–34), signifying the ability to generate broad V1V2 responses could be an important property of an HIV-1 vaccine candidate. We measured binding of serum IgG from 2 weeks post protein boost to gp70-V1V2 scaffold proteins from 16 HIV-1 strains spanning diverse clades by Binding Antibody Multiplex Assay (BAMA) (4), in addition to monitoring this against the challenge virus specific gp70-V1V2 by ELISA. Both routes of immunization induced a strong and broad V1V2-specific response (Fig. 2G). The response to the immunogen (C.1086) V1V2 sequence was comparable between the groups (Fig. 2H right, G) but was marginally higher against the challenge virus V1V2 (2.5 to 4-fold) in the ID/SC group relative to NF-Oral group (Fig. 2H left). Similarly, the ID/SC group displayed significantly higher gp70-V1V2 recognition breadth than the NF-Oral group ($p<0.0001$, Fig. 2I). Immunization via the oral route elicited considerably higher undesirable serum antibodies against the V3 peptide (Fig. 2J) compared to ID/SC. Serum from both immunization regimens showed comparable recognition of membrane anchored full-length env from the challenge virus strain (Fig. 2K).

In summary, the clade C MVA/CycP gp120 protein vaccination delivered via either ID/SC or NF-Oral route induced a strong IgG and IgG1 dominant binding antibody response in rectal secretions and serum. The serum antibodies had broad specificity and potential to bind gp70-V1V2 scaffolds from diverse HIV-1 clades and heterologous tier2 challenge virus env presented on SHIV-transfected cells.

MVA/CycP-gp120 vaccination elicits antibodies with multiple functional activities

We next quantified the ability of serum antibodies to carry out anti-viral functions using a series of functional assays, including neutralization, antibody-dependent cell-mediated virus inhibition (ADCVI), antibody-dependent cellular cytotoxicity (ADCC), antibody-dependent cellular phagocytosis (ADCP, monocyte mediated) and antibody-dependent neutrophil phagocytosis (ADNP). We evaluated the neutralizing antibody responses in serum against pseudoviruses expressing homologous C.1086 and heterologous 1157ipD3N4.G13.10 *envs* using the TZM-bl assay (35). Following a single protein boost, both immunization groups had low levels of neutralization titers against heterologous 1157ipD3N4 *env* G13.10 (mean ID_{50} 40) and no detectable titer (ID_{50} <20) against the homologous C.1086 pseudoviruses (Fig. 3A, table S2). The ADCVI and ADCC effector functions were measured against the challenge virus using SHIV1157ipD3N4 infected CEM-NK^r cells. The ADCVI and ADCC activities were moderate for both immunization groups with geometric mean scores of 19

and 11, respectively (Fig. 3A). In addition, we measured ADCP and ADNP activities of the serum by monitoring the uptake of C.1086 trimer coated fluorescently labelled beads (pre-incubated with serum) by monocytes (ADCP) and neutrophils (ADNP) (36, 37). The serum from both the immunization groups exhibited moderate ADCP (mean 17), and low ADNP (mean 4) scores. None of the measured functional activities were preferentially enhanced by either ID/SC or NF-Oral immunization routes.

To further understand the properties of the serum collected after vaccination, we investigated associations between different functional activities, functions and binding specificities of the serum (Fig. 3B). The neutralizing activity measured against 1157ipD3N4.G13.10 *env* pseudotyped virus showed a direct association with ADCC activity measured against SHIV1157ipD3N4-infected cells (r=0.6, p=0.004) and ADNP activity measured using C.1086 trimer coated beads (r=0.6, p=0.002) (Fig. 3B) suggesting an overlap in antibody specificities targeting these activities. We further probed whether we could associate any Env-specific binding activities with the functional activities. Binding antibodies specific for the C.1086 trimer (r=0.6, p=0.005) and 1157ipD3N4 gp160 (r=0.7, p=0.001) showed strong direct association with neutralizing activity. Additionally, antibodies specific to gp70 V1V2-scaffold showed strong direct association with neutralization (r=0.6, p=0.006), ADCVI (r=0.6, p=0.011) and ADNP (r=0.6, p=0.004) functions (Fig. 3B). This observation was consistent with data from previous studies showing the ability of V1V2-scaffold specific antibodies to be functionally active (38). The env recognition breadth of IgG1 also showed a direct association with ADCVI activity (r=0.6, p=0.007, Fig. 3B). In summary, these data showed that both routes of vaccination induced antibodies with polyfunctional activities and there was a strong association between gp160 or V1V1 scaffold binding activity and multiple functions of the antibody response.

Vaccine induced antibody Fc glycoforms show a distinct glycosylation pattern compared to baseline IgG with reduced fucosylation and bisecting GlcNAc.

The glycosylation profile of IgG Fc region has been reported to modulate various immune responses and play an important role in defining immune pathology in multiple diseases including influenza, HIV-1, tuberculosis, and SARS-CoV-2 (39–41). The route of vaccination has been shown to influence the Fc glycan composition and effect different functional activities (42). We therefore probed whether there was any variability in the Fc glycosylation profile between the ID/SC and NF-Oral immunization groups, and their relationships with different effector activities and antibody sub-classes. The Fc glycosylation profile of Env-specific IgGs elicited in the study after the final immunization was composed of 50% agalactosylated (G0), 10% mono-galactosylated (G1) and 31% di-galactosylated (G2) representing the agalactosylated form being the dominant fraction (Fig. 3, C and E, fig. S4C). In addition, 34% of the Env-specific IgG was fucosylated (F), 17% was sialylated (S) and the bisecting GlcNAc (B) represented a small proportion of 6% (Fig. 3C and fig. S4C). The majority of agalactosylated form of the antibody was neither fucosylated nor with bisecting GlcNAc (Fig. 3D and fig. S4C), in contrast the majority of digalactosylated fraction was fucosylated and/or sialylated with G2F (9.6%), G2S2F (6.8%) and G2S2 (4.5%) (Fig. 3E and fig. S4C). The distribution profile of glycoforms amongst the two

immunization groups was comparable demonstrating that the route of vaccination did not influence the glycosylation pattern of vaccine-induced IgG response (Fig. 3C and fig. S4D).

The Fc glycosylation pattern of Env-specific IgG was markedly distinct from that of total IgG prior to vaccination (baseline, figs. S4A–C and Fig. 3E). The major difference was for fucosylation and bisecting GlcNAc (Fig. 3C). The majority (98%) of baseline IgG was fucosylated as opposed to only 34% of the Env-specific IgG. Similarly, 43% of baseline IgG was bisecting GlcNAc as opposed to only 6% of the Env-specific IgG. The difference for fucosylation and bisecting GlcNAc was most striking for the G0 fraction (fig. S4C). While the total Env-specific G0 fraction was comparable between the two groups (Fig. 3C), the majority of G0 fraction of baseline IgG was fucosylated (99%) and 60% was with bisecting GlcNAc (Fig. 3D and fig. S4C). However, the majority of G0 fraction of Env-specific IgG was without fucosylation and bisecting GlcNAc (Fig. 3D and fig. S4C). Lack of fucosylation of human IgG has been shown to improve binding to FcγRIIIa and ADCC activity of the Ab (43–45). In addition to these differences in the G0 fraction, the total G1 fraction was significantly lower and G2 fraction was marginally higher for Env-specific IgG compared to baseline IgG (Fig. 3C).

To understand if the Fc glycans could influence the functional activities elicited in the study, we observed ADCVI activity to inversely associate with G2S2F fraction (Fig. 3F, $r=-0.6$, $p=0.03$); which agreed with previoiusly reported negative influence of di-galactosylated, fucosylated, sialylated glycoforms in regulating effector functions of HIV-1 specific antibodies (10). Bisecting GlcNAc has been reported to inhibit the addition of fucose to the Fc glycan branch, thereby indirectly improving effector functions (40). In this context, we observed the ADNP activity to directly associate with total bisecting GlcNAc glycoform fraction (Fig. 3F, $r=0.7$, $p=0.005$). The presence of correlative relationships between glycoforms and functional activities, regardless of the antigen specificity of the assays suggested notable contribution of the glycoform for the functions monitored. Network analysis of the significant correlates (spearman's $|r| > 0.7$, $p < 0.05$) between the functions, IgG subtypes and Fc glycoforms displayed association of Env-specific recognition breadth of IgG3 with enhanced ADCVI function, which were associated with reduced G2S2F and di-sialylated Fc glycoforms (fig. S4E, considering NF-Oral group).

In summary, the data showed that MVA/CycP-gp120 vaccine induced env specific antibody with a distinct Fc glycosylation pattern compared to antibody prior to vaccination and specific glycosylation patterns were associated with enhanced effector functions.

Vaccine-induced proliferating CD4$^+$ T cells in blood show lower expression of CCR5, α4β7 and CCR6, and higher expression of CXCR3

To determine the nature of CD4$^+$ T cells induced by MVA/Cyc-gp120 vaccination with respect to expression of markers associated with HIV target cells we characterized the phenotype of proliferating (Ki-67$^+$) CD4$^+$ T cells in the blood for expression of chemokine receptors α4β7 and CCR5 (46, 47) (Fig. 4, A and B). We sampled blood at baseline (pre vaccination bleed), peak and memory time points after each immunization (Fig. 4A). About 2–5% (mean 3.4%) of CD4$^+$ T cells were Ki-67$^+$ prior to immunization and these cells expanded by an average 2.4-fold (4–14%, mean 8%) at day 7 after the second MVA boost,

which further increased by 1.3-fold (6–18%, mean 11%) at day 14 after the protein boost and returned to baseline at week 34 of the study. We characterized the co-expression of α4β7 and CCR5 at the peak effector phase (week 24) since T cells are expected to circulate through blood before they migrate to different tissues at this time point. In our previous study we showed that the frequency of IFNγ+ CD4 T cells at the peak effector phase in blood predict IFNγ+ CD4 T cells in the mucosa several months after vaccination (14). At their peak proliferative phase (week 24), vaccine-induced proliferating cells showed lower frequencies of $\alpha4\beta7^{+}CCR5^{+}$ (net 2-fold reduction, p 0.0015 ID/SC, 0.004 NF-Oral), or $\alpha4\beta7^{+}CCR5^{-}$ (p <0.0001 ID/SC, 0.015 NF-Oral) cells relative to unvaccinated animals (Fig. 4B). This resulted in 1.3-fold (mean) increase in the fraction of Ki-67^{+} $CD4^{+}$ T cells that lacked $\alpha4\beta7^{-}CCR5^{-}$ expression in vaccinated arms (Fig. 4B, p <0.0001 ID/SC, <0.001 NF-Oral) relative to unvaccinated animals. These data demonstrated that the majority of vaccine induced $CD4^{+}$ T cells fail to express HIV infection susceptible α4β7 or/and CCR5 receptors in circulation.

We next investigated if the route of vaccination influenced the T helper polarization by studying co-expression of CXCR3 (Th1), CCR6 (Th17) and CXCR5 (Tfh) chemokine receptors using the Boolean function of Flowjo (Fig. 4C). This analysis revealed that the major fraction of proliferating $CD4^{+}$ T cells in circulation following protein vaccination was Th1 polarized ($CXCR3^{+}CCR6^{-}CXCR5^{-}$). Nearly 27% (mean) of circulating Ki-$67^{+}CD4^{+}$ T cells were CXCR3 single positive at baseline in animals prior to vaccination. At the peak effector phase after vaccination, this fraction was boosted by 1.6-fold (mean) in both groups. In contrast, the proportion of Th17 polarized ($CXCR3^{-}CCR6^{+}CXCR5^{-}$) cells decreased by 2.2 and 1.4-fold in ID/SC and NF-Oral groups respectively, relative to the baseline fraction measured for unvaccinated controls (mean 18%). Similarly, fraction of cells co-expressing CXCR5 and CCR6 (cTfh17) decreased in the vaccinated groups (mean 2.2-fold). Oral immunization induced higher fraction of Th17 polarized cells than parenteral immunization (p=0.0002). The results demonstrated that vaccination predominantly induced Th1 polarized circulating $CD4^{+}$ T cells and oral immunization induced more Th17 cells compared to parenteral vaccination.

Circulating PD-1^{+} $CXCR5^{+}$ $CXCR3^{+}$ memory Tfh cells have been shown to correlate with induction of neutralizing antibody responses in HIV (48) and HCV infected patients (49). Similarly, blood $ICOS^{+}$ $CXCR5^{+}$ $CXCR3^{+}$ $CD4^{+}$ T cells have been shown to correlate with the development of antibody responses upon seasonal influenza vaccination in humans (50) and generation of high avidity antibody with longer persistence following protein vaccination in rhesus macaques (51). Interestingly, the MVA/CycP-gp120 vaccine-induced circulating Tfh or cTfh ($CXCR5^{+}$PD-1^{+}) correlated positively with antibody effector functions (neutralization and ADCP scores) and Env-specific binding antibody responses (figs. S5, A and B). Similar correlations were also observed with $CXCR3^{+}$ cTfhs (fig. S5B). These data suggested that MVA-HIV/CycP-gp120 vaccination induced cTfh contributed significantly for the enhanced function of the antibody response.

Protein boost in the presence of dmLT induced TNFα producing CD4+ T cells in blood and rectum

We next examined SHIV specific $CD4^+$ and $CD8^+$ T cell responses in blood and in the rectal mucosa after immunization by stimulating cells with 15-mer overlapping peptide pools (overlapping by 11aa) specific to SIVmac239 Gag and C.1086 env sequences, and measuring the expression of IFNγ and TNFα by flow cytometry (Fig. 4D and figs. S5, C and D). Immunizations resulted in modest non-uniform production of SHIV-specific IFNγ in $CD4^+$ T cells in blood, with peak responses measured one week after the second MVA (week 11) and similar responses across both immunization arms (fig. S5D). The IFNγ responses were not further boosted after the protein immunization, despite increase in proliferating circulating Th1 polarized CD4+ T cells after protein boost (fig. S5D, Fig. 4C). We did not observe any increase in SHIV-specific $IFN\gamma^+$ $CD4^+$ T cells in the rectal mucosa during the study. However, SHIV-specific TNFα producing $CD4^+$ T cells in blood expanded to mean of 0.1% (range 0.03–0.6% ID/SC, 0.03–0.14% NF-Oral, fig. S5D) after the protein boost. Similarly, TNFα+ CD4 T cells also expanded in the rectal tissue of vaccinated animals (0.6% mean, 0.3–1.6%) at 2 weeks following protein boost (fig. S5D). At pre challenge, mucosal consensus C SHIV specific TNFα producing CD4+ T cell responses were higher in the vaccine groups relative to unvaccinated animals (Fig. 4D) and were similar between the two immunization groups.

Unlike $CD4^+$ responses, SHIV-specific $CD8^+$ T cell responses were overall low and were not higher than pre-vaccination background levels in blood (fig. S5D). At pre-challenge, vaccinated animals showed higher frequencies of $IFN\gamma^+$ and $TNF\alpha^+$ CD8 T cell responses in rectum relative to unvaccinated animals, with no difference in responses between the two immunization groups (Fig. 4D). In summary, protein boosting in the presence of dmLT as adjuvant primarily induced SHIV-specific TNFα producing $CD4^+$ and $CD8^+$ T cell responses in the rectum at pre challenge.

MVA-HIV/cycP-gp120 vaccination protects rhesus macaques from mucosal SHIV challenge and controls viral replication irrespective of the immunization route

To evaluate the efficacy of the clade C based MVA-HIV/cycP-gp120 vaccine, we challenged animals 16 weeks after the protein boost with repeated low dose weekly intra-rectal inoculation with heterologous clade C tier2 SHIV 1157ipD3N4 (Fig. 2A). Both vaccinated groups showed significant protection from infection (p=0.02 for both groups, log-rank Mantel-Cox test, Fig. 5A), with 40% animals remaining uninfected (4 in each group) after the final challenge. The efficacy of the vaccine per exposure was calculated to be 67.7%, 95% [CI] 23.5 to 86.4; p=0.02 for both ID/SC and NF-Oral immunization groups (Fig. 5B). Ability of the vaccine to control the infection or reduce viral burden defines another important readout of vaccine efficacy. We therefore measured viral RNA copies in the plasma of vaccinated and unvaccinated infected animals on weeks 1, 2, 3, 6 and 12 after infection (Fig. 5C). The vaccinated arms displayed a significant reduction in viral RNA copies throughout the time-points monitored, beginning as early as week 2 after infection relative to the unvaccinated controls; and also when viral load AUCs (area under the curve) were compared (Fig. 5, C and D). At week 2 post infection, the ID/SC and NF-Oral groups displayed 62-fold, and 11-fold reduction in viral load respectively (ID/SC 8×10^4, NF-Oral

5×10^5 geomean RNA copies/ml) relative to the unvaccinated animals (geomean 5×10^6 RNA copies/ml). Interestingly, following week 6 of infection, the NF-Oral group displayed the highest (74-fold) reduction in viral load relative to controls, when the ID/SC group displayed 23 to 32-fold reduction in viral load. By week 12, all animals showed significant reduction in viral load relative to their peak, however, the RNA copies measured in the vaccinated groups were markedly lower (ID/SC 9×10^2, NF-Oral 4×10^2 unvaccinated 3×10^4 RNA copies/ml) than the unvaccinated animals, indicating the capacity of the vaccines to elicit immune responses that contribute to the control of viral burden. In addition, vaccinated animals that became infected earlier during the challenges had higher viral loads than those that became infected later (Fig. 5E), suggesting that factors contributing towards delaying infection may also be important for controlling the viral burden. In summary, MVA-HIV/cycP-gp120 vaccination protected rhesus macaques from mucosal tier2 Clade C SHIV challenge and controlled viral replication irrespective of the immunization route.

Vaccine specific humoral and T cell responses are associated with protection and reduced viral replication after mucosal SHIV challenge

We performed correlative analyses to identify immune features that likely contributed to protection in vaccinated animals (Figs. 6A–D). We focused our analyses on vaccine-induced antibody responses in serum and rectal secretions, cytokine positive $CD8^+$ and $CD4^+$ T cells in blood and rectum, and total proliferating $CD4^+$ T cells. A higher fraction of Env-specific IgG with Fc glycoform G1FB correlated with delayed acquisition ($r=0.7$, $p=0.005$), while the presence of a higher fraction of G2S2F glycoform correlated with earlier acquisition ($r=-0.6$, $p=0.022$), indicating that specific Fc glycoform composition was associated with protection (Fig. 6A). The frequencies of Consensus C Env-specific $CD8^+$ T cells producing TNFα and IFNγ in rectum (site of virus exposure) at pre-challenge were associated with delayed acquisition (Fig. 6B, $r=0.6$, $p=0.005$). We further classified animals into either early infected (≤3 challenges, n=9) or late infected/protected (≥4 challenges, n=11) and compared the kinetics of expansion of Ki-67^+ $CD4^+$ T cells after each vaccination. Animals that got infected early during the challenge phase showed marked expansion of proliferating $CD4^+$ T cells following each vaccination that peaked at 2 weeks after the protein vaccination. However, animals that got infected later during the challenge phase or protected showed only a small increase after each vaccination and exhibited 2-fold lower Ki-67^+ $CD4^+$ T cells (14% in early infected vs 7% in late infected/protected) at week 24 compared to early infected animals (Fig. 6C). With respect to vaccine-specific $CD4^+$ T cells, the consensus C Env-specific $CD4^+$ T cells producing TNFα in rectum at pre-challenge were present at higher levels in protected compared to infected animals, unlike cells producing IFNγ which did not show any difference (Fig. 6D, TNFα+ $p=0.04$, IFNγ+ $p=0.92$). To understand the mechanism behind this, we measured expression of CCR5 on mucosal $CD4^+$ T cells producing TNFα or IFNγ after in-vitro stimulation with PMA/Ionomycin. We observed that $TNF\alpha^+$ $CD4^+$ T cells express significantly lower CCR5 (both as a fraction and mean fluorescence intensity per cell) compared to $IFN\gamma^+$ $CD4^+$ T cells (Fig. 6E) making the former less potential targets for viral infection. We could not perform this analysis on Env-specific $CD4^+$ T cells owing to their low frequency. We further evaluated potential correlations between peak viral load and antigen-specific cellular and humoral responses to predict factors controlling viral replication (Figs. 6 F and G). The ADCVI activity measured

against the challenge virus (Fig 6F, r=−0.6, p=0.046) and 1157ipD3N4 V1V2-scaffold specific responses (Fig 6G, r=−0.6, p=0.040) at the peak of antibody response (week 24) were associated with reduced viral load. As described above (Fig. 3F), we observed serum samples with low Env-specific G2S2F fraction to show significantly higher ADCVI activity compared to samples with high G2S2F fraction. These results suggested that Env-specific reduced G2S2F Fc glycoform associated with protection (Fig. 6A) could also have played an important role in controlling viral burden via enhanced ADCVI activity.

In summary, Env-specific IgG in serum with distinct Fc glycoforms (higher fraction of G1FB and lower fraction of G2S2F), vaccine induced mucosal $TNF\alpha^+IFN\gamma^+$ $CD8^+$ T cells, $TNF\alpha^+$ $CD4^+$ T cells displaying low CCR5 viral co-receptor expression at pre-challenge contributed towards protection in the study. Additionally, animals exhibiting low proliferating blood $CD4^+$ T cells were associated with delayed infection.

Discussion

Clade C subtype specific HIV-1 infections are responsible for a large proportion (~48%) of global HIV-1 burden (52), requiring a vaccine that is effective against these variants. Here we aimed to generate a clade C vaccine that can provide heterologous protection against a pathogenic intrarectal SHIV infection and define immune correlates for protection in rhesus macaques. In parallel, we also compared the vaccine efficacy following oral (mucosal route) or parenteral (ID for MVA and SC for protein) immunization routes. Our results demonstrate that the clade C MVA/CycP-gp120 vaccine provides significant protection from acquisition of heterologous mucosal SHIV infection and control of virus replication in infected animals. We observed significant protection despite the absence of high titer neutralizing activity against the challenge virus. Immune correlate analysis revealed that reduced risk of infection was associated with distinct Fc glycosylation profile of vaccine induced polyfunctional antibodies and T helper response that is resistant to HIV-1 infection. Furthermore, these correlates were not dependent on mucosal or parenteral routes of immunization. We think the protection observed against SHIV 1157ipD3N4 infection in the current study is notable since this is a highly mucosally transmissible tier2 R5 tropic virus, induces high viral set points in macaques and thus represents a stringent challenge virus to evaluate vaccine efficacy (53). Previous challenge studies using this virus in NHPs demonstrated limited vaccine efficacy except a study by Om et al that reported good vaccine protection in male but not female macaques (54–58).

An interesting finding of our study was that MVA/CycP-gp120 vaccination induced Env-specific IgG with a distinct glycosylation pattern that was different from glycosylation of total IgG at baseline, and identified specific associations between Fc glycosylation and enhanced protection from infection. We showed significant associations between higher fraction of Env-specific G1FB and lower fraction of G2S2F glycoforms with reduced risk of infection. It was interesting to note that a previous study by Vaccari et al also showed the presence of higher fraction of G1F and lower fraction of fucosylated G2 forms (G2FB, G2F and G2S1F) in animals that were vaccinated with alum compared to MF59 using ALVAC prime/protein boost strategy (59). While Vaccari et al did not report a direct association between specific Fc glycoform and protection, the alum adjuvanted animals showed better

protection compared to MF59 adjuvanted animals in their study further strengthening the finding about the influence of Fc glycosylation on vaccine protection against SIV and the potential beneficial role of G1FB glycoform and negative influence of G2 forms.

The mechanisms by which Fc glycoforms influence protection needs further investigation. One explanation is that Fc glycosylation influenced the effector function of antibody responses. Towards this, our data showed an inverse association between G2S2F glycoform and ADCVI activity. Mechanistically, lack of fucosylation of human IgG has been reported to improve binding to FcγRIIIa (43–45) and thus could have resulted in better ADCVI function of the antibody. We hypothesized that we would identify additional associations between Fc glycosylation pattern and other functional activities such as neutralization and ADCC, but this was not the case. We think this may be because we used C.1086 Env trimer for Fc glycan profile and 1157 Env or challenge virus (1157ipD3N4) for functional assays. Unfortunately, we couldn't use 1157 Env for glycan analysis since we didn't have a trimer protein for this Env. The mechanisms by which the vaccination influences glycosylation is still under active investigation. Various factors including the route, number of immunizations and adjuvants can influence antibody glycosylation (60, 61). Towards this, it will be important to investigate the influence of dmLT adjuvant on Fc glycosylation and protection.

Although we observed an association between G2S2F glycoform and ADCVI activity or protection, we did not observe an association between ADCVI activity and protection and thus could not establish a mechanistic link between G2S2F glycoform and protection. The lack of association between ADCVI activity and protection in this study was different compared to our previous studies where we observed a direct association between ADCVI activity and protection (25, 62, 63). However, in this study we observed a strong direct association between ADCVI activity and viral control. Furthermore, animals that became infected later during the challenge phase showed better viral control. This raised the possibility that ADCVI activity could have contributed to blunting of local virus replication soon after infection leading to non-productive infection and better prevention of infection.

Previous studies showed an association between higher frequencies of total activated CD4 T cells or $\alpha4\beta7^+$ Ki-67^+ CD4 T cells and enhanced acquisition of SIV infection in macaques (64–66). In our study we seggregated vaccinated animals into early or late (or protected) acquires of infection based on their infection status during the challenge phase, and observed maximum difference between the groups in terms of proliferation of circulating $CD4^+$ T cells at peak CD4 T cell response (two weeks after the protein boost). We used this time point since this represented peak effector phase following booster vaccination at which T cells are expected to circulate through blood before they migrate to different tissues. In addition, in our previous study we showed that the frequency of IFNγ^+ CD4 T cells at the peak effector phase in blood predict IFNγ^+ CD4 T cells in the mucosa several months after vaccination (14). The differences in Ki-67 expression in these two acquisition groups do not persist at pre-challenge (12 weeks after the boost) as cells that migrated to tissue at the peak effector phase do not recirculate through blood.

It is becoming increasingly clear that that the HIV susceptible phenotype of vaccine induced CD4 T cells can significantly modulate vaccine protection especially under conditions of poor neutralizing antibody response, and the phenotype of CD4 T helper response can be influenced by the vector platform and the adjuvants used (14, 65, 67). In this study we showed a positive association between vaccine-induced TNFα producing CD4 T cells in the rectum and better protection from infection, pointing to a mechanism in which TNFα producing CD4 T cells express lower CCR5 compared to IFNγ producing CD4 T cells. These results highlight the need for comprehensively screening for the HIV susceptible phenotype of CD4 T cell helper response induced by different adjuvants.

While we observed an increase in circulating $Ki67^+$ $CXCR3^+$ (Th1) CD4 T cells after the protein boost, we measured very low cytokine responses by intracellular cytokine staining. However, not all proliferating cells during the peak of response might produce cytokines such as IFNγ and TNFα following stimulation with specific peptides. This has been a limitation in defining antigen-specific Tfh responses and the field has resorted to doing the AIM assay (68). In addition, there might be bystander proliferation of non-vaccine specific cells. Despite these limitations, we followed these cells to get a broad understanding of overall nature of responding cells following vaccination since HIV-1 can also infect non-HIV specific CD4 T cells.

Mucosal immune responses are generally more efficiently induced by mucosal vaccinations than by the parenteral route of immunization (16). However, we did not observe differences in vaccine elicited antibody architecture in mucosal secretions between the oral and parenteral vaccination arms. This could be due to the use of the strong mucosal adjuvant dmLT in both immunization routes driving similar mucosal responses. Yet, we did not observe IgA responses in mucosal secretions in either vaccination arms. In our previous pilot study(25), oral immunization induced strong Env-specific IgA responses in vaginal secretions and modest levels in rectal secretions using high dose of 50μg dmLT as adjuvant. We did not measure IgA in vaginal secretions in the current study since we used all male animals. It will be interesting to measure the induction of mucosal IgA responses with a higher concentration of adjuvant (current study used 5μg dmLT) using the Clade C specific MVA/CycP-gp120 vaccine regimen administered orally and determine its impact on the protection outcome. Although high serum IgA levels have been linked to increased risk of infection in the RV144 trial (2), mucosal IgA (dimeric form) has different features than serum IgA (monomeric form) and passive mucosal administration of Env-specific mAbs as dimeric IgA have been shown to provide protection against mucosal transmission of SHIV (69).

Th17 cells are largely enriched in gut and express CCR6 as the trafficking receptor to tissue microenvironments of the intestine such as Payer's patches (70). It was encouraging to see that the mucosal immunization resulted in higher expression of $CCR6^+CXCR3^-$ (Th17 polarized) chemokine receptors on proliferating $CD4^+$ T cells, indicating enhanced mucosal trafficking of T cells following oral immunization. In another study (42), the authors demonstrated that a DNA/rAd5-SIVmac239 based vaccine regimen administered to NHPs via either intramuscularly (IM), or by aerosol (AE) route, conferred similar levels of protection. However, it resulted in differential induction of Env-specific Fc glycoforms,

and effector functions (IM preferentially induced IgG driven ADCP while AE elicited IgA driven ADNP) as correlates of reduced infection risk. We did not observe any quantitative differences in any antigen-specific antibodies and functions in either immunization groups, with no major differences in any protection correlates between the two groups/immunization routes.

The use of needle-free injectors for drug delivery over traditional syringes and hypodermic needles are attractive due to their ease of use for mass immunizations, avoiding needle-stick injuries, and issues with re-use of a needle (71–73). PharmaJet has been approved to be safe and effective in delivering vaccines/immunogens related to influenza, MMR, IPV, HPV, Zika, and recently SARS-CoV-2 related DNA vaccine in an ongoing PhaseIII clinical trial (74–76). We have successfully demonstrated the effectiveness of MVA/CycP-gp120 HIV-1 vaccines delivered by the needle-free jet injectors Syrijet Mark II (Keystone Industries, Cherry Hill, New Jersey, United States) (25) and PharmaJet (current study). The equivalent protection levels and immune profiles observed when the vaccines were delivered either using the jet injector (NF-Oral group) or hypodermic needle (ID/SC group) suggests retention of the properties of the immunogens delivered using the needle-free injector. We anticipate future vaccine delivery methods to adopt the benefits of using quick, hassle-free and painless needle-free injectors.

In the current study we performed a maximum of six weekly intra-rectal challenges to evaluate vaccine efficacy. While these results are highly encouraging, increasing the number of challenges to 12 would further increase the rigor of the results. Additionally, our results showed that animals with higher proliferating $CD4^+$ T cells during vaccination displayed increased rate of acquisition of SHIV infection. However, we did not monitor for proliferating CD4 T cells at the end of all six challenges. This information would have allowed us to establish if there was any relationship between proliferating CD4 T cell frequency post challenge and infection status. Furthermore, defining the association between Env-specific antibody Fc glycosylation at additional time points during vaccination and acquisition of infection would strengthen immune correlates for protection.

In conclusion, our results validated the protective efficacy of the MVA/cycP-gp120 immunization regimen against a pathogenic heterologous clade C SHIV challenge and identified important immune correlates related to antibody glycosylation and T cell responses highlighting the potential utility of this vaccine to offer protection against diverse strains of HIV-1. The 68% vaccine efficacy observed in this study is likely to have some impact on annual new infections based on modeling done by Harmon et al., that estimated a HIV vaccine with 70% efficacy would reduce annual new infections by 78% (67).

Materials and methods

Study design

The goal of this study was to determine (a) the protective efficacy of an optimized HIV-1 Clade C MVA/CycP-gp120 trimer vaccine with dmLT mucosal adjuvant against heterologous pathogenic SHIV in macaques, (b) whether altering the route of immunization would influence the protection outcome and immune responses, and (c) identify the immune

correlates of protection. To address these, we first designed, characterized multiple Clade C CycP gp120 constructs, and selected the one efficiently folding into trimers exhibiting higher binding to trimer specific bnAbs as the protein component of the vaccine regimen. Details of the immunogens, purification and characterization have been described in Supplementary Materials and Methods. Male Indian rhesus macaques *Macaca mulatta* (n=20, 3.5–5.6 years old, mean 4.2 years, mean 6.4kg body weight, 4.3–9.7kg) used in the study were housed in pairs in standard NHP cages at Yerkes National Primate Research Center, and fed with standard primate food (Purina monkey chow), fresh fruit, and enrichment daily, with free access to water. 29 of the 30 animals were *Mamu A*01*$^{-}$. All immunizations, blood draws and sample collections were performed under anesthesia with ketamine (5–10mg/kg) or telazol (3–5mg/kg) by trained research and veterinary staff who were blinded for study group information. All vaccinated animals were divided into two groups (n=10 per group) i.e., ID/SC and NF-Oral. The animals were primed with MVA expressing HIV-1 C.1086-VLP (1×10^8 pfu in 100μl per dose) at weeks 0 and 10, followed by boosting with ConC-C CycP gp120 (100μg/dose with 5μg dmLT adjuvant (26)) at week 22. The ID/SC group received MVA via intradermal route and protein via subcutaneous route, dose split equally between right and left thigh. The NF-Oral group received both vaccines in the mouth by PharmaJet Tropis needle-free injection (PharmaJet, Inc.) with total dose split between buccal and sublingual sites. Ten age, sex and weight matched *Mamu-A*01*$^{-}$ animals were used as unvaccinated controls after all immunizations were done. All vaccinated and un-vaccinated animals were challenged weekly intra-rectally with SHIV1157ipD3N4 (NIH AIDS reagents program, cat# 11689 (53), 1:700 dilution of stock (containing 9.8×10^6 50% tissue culture infective doses [$TCID_{50}$]/ml and 257 ng/ml p27) beginning week 38 for a maximum of 6 challenges or until two consecutive positive viral load (RNA copies/ml measured in plasma by quantitative RT-PCR as described earlier (77) >60). To determine peak and set-point viral load, plasma viral loads were monitored for upto 12 weeks post infection.

Ethics statement

All experiments involving rhesus macaques were conducted at Yerkes National Primate Research Center in compliance with Emory University Institutional Animal Care and Use Committee (IACUC) protocol YER2003491, under USDA regulations and *Guide for the Care and Use of Laboratory Animals* guidelines.

Assays to characterize antigen specific serum properties

ELISA was performed to determine C.1086 trimer (UFO-v2-RQY^{173} (28)), Conc-CycP gp120 trimer, gp70 1157 V1V2, gp70 C.1086 V1V2-specific binding antibodies in serum and avidity of antibodies against SHIV 1157ipD3N4 VLPs; Binding antibody multiplex assay (BAMA) to measure serum binding antibodies against a diverse panel of gp70 V1V2 envs, and antigen-specific antibodies in secretions. Binding of rhesus serum to full-length 1157ipD3N4 challenge virus env membrane anchored and expressed on HEK293T cells was measured. Functional assays were performed and included neutralization against pseudotyped C.1086 K160N, 1157ipD3N4 Env G13.10 envs by TZM-bl assay, ADCVI and ADCC against the challenge virus using CCR5^{+} CEM NK^{r} SHIV infected cells as target cells and human PBMCs, rhesus CD16 expressing KHYG1 NK cells as effector

cells respectively, ADNP and ADCP against target beads coated with C.1086 trimer using human neutrophils and THP-1 cells as effector cells respectively. Antigen-specific antibody subclass/isotypes were identified by Luminex multiplexing. C.1086 trimer specific IgG Fc glycosylation analysis was performed by capillary electrophoresis. C.1086 trimer used in the study refers to C.1086 UFO-v2-RQY^{173} (28). Details of all the assays have been mentioned in Supplementary Materials and Methods.

Intracellular-cytokine staining (ICS) assay and flow-cytometry based phenotypic characterization of immune cells

PBMCs and cell suspensions obtained from processed rectal biopsies (as previously described (25)) were stimulated with SIVmac239 Gag and HIV C.1086 Env peptides (2μg/ml each) (NIH AIDS Reagent program) in presence of co-stimulatory anti-CD28 (BD) and anti-CD49d (BD) (1μg/ml each) for 2 hrs at 37^{o}C, 5% CO_2 as previously described (25). Protein transport inhibitors GolgiStop (BD) and GolgiPlug (BD) were added (0.5μg/ml each) and incubated for additional 4hrs, followed by staining of cells to measure SHIV specific cellular production of cytokines (IFN-g, TNF-α, IL-2) by flow-cytometry. All response values (say, A, if A< (0.02 for analyses of rectal samples or 0.01 for analyses of PBMCs), A=0 and also, if A< (2* Response measured for their unstimulated controls, say B), A=0) were subtracted from values measured using their un-stimulated controls, B. The net subtracted response values used for analyses (Y, where Y>0) = A – B. For phenotypic characterization of cells, PBMCs were stained for following phenotypic markers (clone of antibodies used): CD3 (SP34–2), CD4 (SK3), CD8 (RPA-T8), CD45RA (5H9), CCR7 (150503), CXCR5 (MU5UBEE), CCR5 (3A9), CCR6 (11A9), CXCR3 (G025H7), α4β7 (NHP reagent resource), live/dead fixable stain and intracellular staining for Ki67 (B56). Visualization and analyses of flow-cytometry stains were done using FlowJo v9.9.6 software. Additional details of the staining method and antibodies used have been described in Supplementary Materials and Methods.

Network visualization and multivariate analyses

All significant correlations (spearman's correlation coefficient | r | >0.7, and two-sided p<0.05) were used to visualize as network using Cytoscape 3.8.2 (78). Principal Component Analyses (PCA) analyses was performed using *PCA()*, *FactoMineR* package in R v3.5.2 (79).

Statistical Analyses

All statistical analyses were performed using GraphPad Prism v9 software. Statistical significance between groups was performed by Mann-Whitney U test. Wilcoxon matched-pairs signed rank test, two-tailed was performed for statistical comparison within groups. For comparisons involving multiple groups, One way ANOVA test was performed followed by Mann-Whitney U test for statistical comparison between groups. In all cases Bonferroni's correction for multiple comparisons was done and p values found significant after correction reported. Spearman's correlation coefficients were calculated for measuring correlations and two-sided p values indicated; all significant findings after adjusting for multiple comparisons by Bonferroni correction reported. Kaplan-Meier curves and log-rank Mantel Cox test were used to display and estimate differences in rate of acquisition of infection

between vaccinated and control unvaccinated groups. *p < 0.05, **p< 0.01, ***p<0.001, ****p<0.0001.

Supplementary Material

Refer to Web version on PubMed Central for supplementary material.

Acknowledgements

We thank Stephanie Ehnert, Christopher Souder, Dara Johnston, John Wambua, other members of Yerkes Research Resources and the Yerkes veterinary staff for animal care and sampling, Shan Liang and Shelly Wang and the CFAR Immunology Core for plasma viral load assays; Kiran Gill, Barbara Cervasi and CFAR Immunology Core for maintenance of flow cytometers. We thank Lu Zhang and Tiffany Peters (Duke University, USA) for their expert assistance with BAMA experiments and analyses. We thank Drs Bernard Moss and Linda Wyatt at NIH for pLW73 vector and rMVA expressing SIVmac239 gag and pol genes; Dr. Ruth Ruprecht and the HIV reagent resource for generously providing SHIV1157ipD3N4; Dr. Abraham Pinter (Rutgers Medical School) for gp70 1157 V1V2 protein, Dr. Jim Hoxie (University of Pennsylvania) for $CCR5^{+}$ CEM-NK^{r} cells used in ADCVI assay, Dr. David Evans (University of Wisconsin, Madison) for $CCR5^{+}$ CEM NK^{r} cells encoding a tat-inducible luciferase promoter and KHYG1 NK effector cells (expressing rhesus CD16) used in ADCC assay. We are extremely thankful to Dr. Du Yuhong (Emory University) for letting use the Octet RED384 instrument for the BLI experiments. We thank Emory Glycomics and Molecular Interactions Core (EGMIC) for glycan labeling and LC/MS analysis support and Dr Blaine Russell Roberts (Emory University) for his valuable suggestions related to mass-spectrometry specific data analyses. We thank Dr. Robert Sonowal (Emory University, GA) for his valuable suggestions.

Funding

This work was supported in part by National Institutes of Health (NIH) Grants R01DE026333 (R.R.A), R01AI148378 (R.R.A) and R01AI128837 (C.D); Office of research Infrastructure Programs (ORIP/NIH) base grant P51 OD011132 (ENPRC), NIH Primate Contract HHSN27201100016C (G.D.T), Duke CFAR P30 AI064518 (G.D.T).

References

1. Yates NL, Liao HX, Fong Y, deCamp A, Vandergrift NA, Williams WT, Alam SM, Ferrari G, Yang ZY, Seaton KE, Berman PW, Alpert MD, Evans DT, O'Connell RJ, Francis D, Sinangil F, Lee C, Nitayaphan S, Rerks-Ngarm S, Kaewkungwal J, Pitisuttithum P, Tartaglia J, Pinter A, Zolla-Pazner S, Gilbert PB, Nabel GJ, Michael NL, Kim JH, Montefiori DC, Haynes BF, Tomaras GD, Vaccine-induced Env V1-V2 IgG3 correlates with lower HIV-1 infection risk and declines soon after vaccination. Sci Transl Med 6, 228ra239 (2014).
2. Haynes BF, Gilbert PB, McElrath MJ, Zolla-Pazner S, Tomaras GD, Alam SM, Evans DT, Montefiori DC, Karnasuta C, Sutthent R, Liao HX, DeVico AL, Lewis GK, Williams C, Pinter A, Fong Y, Janes H, DeCamp A, Huang Y, Rao M, Billings E, Karasavvas N, Robb ML, Ngauy V, de Souza MS, Paris R, Ferrari G, Bailer RT, Soderberg KA, Andrews C, Berman PW, Frahm N, De Rosa SC, Alpert MD, Yates NL, Shen X, Koup RA, Pitisuttithum P, Kaewkungwal J, Nitayaphan S, Rerks-Ngarm S, Michael NL, Kim JH, Immune-correlates analysis of an HIV-1 vaccine efficacy trial. N Engl J Med 366, 1275–1286 (2012). [PubMed: 22475592]
3. Rerks-Ngarm S, Pitisuttithum P, Nitayaphan S, Kaewkungwal J, Chiu J, Paris R, Premsri N, Namwat C, de Souza M, Adams E, Benenson M, Gurunathan S, Tartaglia J, McNeil JG, Francis DP, Stablein D, Birx DL, Chunsuttiwat S, Khamboonruang C, Thongcharoen P, Robb ML, Michael NL, Kunasol P, Kim JH, Investigators M-T, Vaccination with ALVAC and AIDSVAX to prevent HIV-1 infection in Thailand. N Engl J Med 361, 2209–2220 (2009). [PubMed: 19843557]
4. Zolla-Pazner S, deCamp A, Gilbert PB, Williams C, Yates NL, Williams WT, Howington R, Fong Y, Morris DE, Soderberg KA, Irene C, Reichman C, Pinter A, Parks R, Pitisuttithum P, Kaewkungwal J, Rerks-Ngarm S, Nitayaphan S, Andrews C, O'Connell RJ, Yang ZY, Nabel GJ, Kim JH, Michael NL, Montefiori DC, Liao HX, Haynes BF, Tomaras GD, Vaccine-induced IgG antibodies to V1V2 regions of multiple HIV-1 subtypes correlate with decreased risk of HIV-1 infection. PLoS One 9, e87572 (2014). [PubMed: 24504509]

5. Zolla-Pazner S, Alvarez R, Kong XP, Weiss S, Vaccine-induced V1V2-specific antibodies control and or protect against infection with HIV, SIV and SHIV. Curr Opin HIV AIDS 14, 309–317 (2019). [PubMed: 30994501]

6. Corey L, Gilbert PB, Tomaras GD, Haynes BF, Pantaleo G, Fauci AS, Immune correlates of vaccine protection against HIV-1 acquisition. Sci Transl Med 7, 310rv317 (2015).

7. Vidarsson G, Dekkers G, Rispens T, IgG subclasses and allotypes: from structure to effector functions. Front Immunol 5, 520 (2014). [PubMed: 25368619]

8. Chung AW, Ghebremichael M, Robinson H, Brown E, Choi I, Lane S, Dugast AS, Schoen MK, Rolland M, Suscovich TJ, Mahan AE, Liao L, Streeck H, Andrews C, Rerks-Ngarm S, Nitayaphan S, de Souza MS, Kaewkungwal J, Pitisuttithum P, Francis D, Michael NL, Kim JH, Bailey-Kellogg C, Ackerman ME, Alter G, Polyfunctional Fc-effector profiles mediated by IgG subclass selection distinguish RV144 and VAX003 vaccines. Sci Transl Med 6, 228ra238 (2014).

9. Reusch D, Tejada ML, Fc glycans of therapeutic antibodies as critical quality attributes. Glycobiology 25, 1325–1334 (2015). [PubMed: 26263923]

10. Ackerman ME, Crispin M, Yu X, Baruah K, Boesch AW, Harvey DJ, Dugast AS, Heizen EL, Ercan A, Choi I, Streeck H, Nigrovic PA, Bailey-Kellogg C, Scanlan C, Alter G, Natural variation in Fc glycosylation of HIV-specific antibodies impacts antiviral activity. J Clin Invest 123, 2183–2192 (2013). [PubMed: 23563315]

11. Offersen R, Yu WH, Scully EP, Julg B, Euler Z, Sadanand S, Garcia-Dominguez D, Zheng L, Rasmussen TA, Jennewein MF, Linde C, Sassic J, Lofano G, Vigano S, Stephenson KE, Fischinger S, Suscovich TJ, Lichterfeld M, Lauffenburger D, Rosenberg ES, Allen T, Altfeld M, Charles RC, Ostergaard L, Tolstrup M, Barouch DH, Sogaard OS, Alter G, HIV Antibody Fc N-Linked Glycosylation Is Associated with Viral Rebound. Cell Rep 33, 108502 (2020). [PubMed: 33326789]

12. Lofano G, Gorman MJ, Yousif AS, Yu WH, Fox JM, Dugast AS, Ackerman ME, Suscovich TJ, Weiner J, Barouch D, Streeck H, Little S, Smith D, Richman D, Lauffenburger D, Walker BD, Diamond MS, Alter G, Antigen-specific antibody Fc glycosylation enhances humoral immunity via the recruitment of complement. Sci Immunol 3, (2018).

13. Collins DR, Gaiha GD, Walker BD, CD8(+) T cells in HIV control, cure and prevention. Nat Rev Immunol 20, 471–482 (2020). [PubMed: 32051540]

14. Chamcha V, Reddy PBJ, Kannanganat S, Wilkins C, Gangadhara S, Velu V, Green R, Law GL, Chang J, Bowen JR, Kozlowski PA, Lifton M, Santra S, Legere T, Chea LS, Chennareddi L, Yu T, Suthar MS, Silvestri G, Derdeyn CA, Gale M Jr., Villinger F, Hunter E, Amara RR, Strong TH1-biased CD4 T cell responses are associated with diminished SIV vaccine efficacy. Sci Transl Med 11, (2019).

15. Veazey RS, DeMaria M, Chalifoux LV, Shvetz DE, Pauley DR, Knight HL, Rosenzweig M, Johnson RP, Desrosiers RC, Lackner AA, Gastrointestinal tract as a major site of CD4+ T cell depletion and viral replication in SIV infection. Science 280, 427–431 (1998). [PubMed: 9545219]

16. Neutra MR, Kozlowski PA, Mucosal vaccines: the promise and the challenge. Nat Rev Immunol 6, 148–158 (2006). [PubMed: 16491139]

17. Belyakov IM, Hel Z, Kelsall B, Kuznetsov VA, Ahlers JD, Nacsa J, Watkins DI, Allen TM, Sette A, Altman J, Woodward R, Markham PD, Clements JD, Franchini G, Strober W, Berzofsky JA, Mucosal AIDS vaccine reduces disease and viral load in gut reservoir and blood after mucosal infection of macaques. Nat Med 7, 1320–1326 (2001). [PubMed: 11726972]

18. Enose Y, Ui M, Miyake A, Suzuki H, Uesaka H, Kuwata T, Kunisawa J, Kiyono H, Takahashi H, Miura T, Hayami M, Protection by intranasal immunization of a nef-deleted, nonpathogenic SHIV against intravaginal challenge with a heterologous pathogenic SHIV. Virology 298, 306–316 (2002). [PubMed: 12127792]

19. Amara RR, Villinger F, Altman JD, Lydy SL, O'Neil SP, Staprans SI, Montefiori DC, Xu Y, Herndon JG, Wyatt LS, Candido MA, Kozyr NL, Earl PL, Smith JM, Ma HL, Grimm BD, Hulsey ML, Miller J, McClure HM, McNicholl JM, Moss B, Robinson HL, Control of a mucosal challenge and prevention of AIDS by a multiprotein DNA/MVA vaccine. Science 292, 69–74 (2001). [PubMed: 11393868]

20. Iyer SS, Gangadhara S, Victor B, Shen X, Chen X, Nabi R, Kasturi SP, Sabula MJ, Labranche CC, Reddy PB, Tomaras GD, Montefiori DC, Moss B, Spearman P, Pulendran B, Kozlowski

PA, Amara RR, Virus-Like Particles Displaying Trimeric Simian Immunodeficiency Virus (SIV) Envelope gp160 Enhance the Breadth of DNA/Modified Vaccinia Virus Ankara SIV Vaccine-Induced Antibody Responses in Rhesus Macaques. J Virol 90, 8842–8854 (2016). [PubMed: 27466414]

21. Goepfert PA, Elizaga ML, Sato A, Qin L, Cardinali M, Hay CM, Hural J, DeRosa SC, DeFawe OD, Tomaras GD, Montefiori DC, Xu Y, Lai L, Kalams SA, Baden LR, Frey SE, Blattner WA, Wyatt LS, Moss B, Robinson HL, A. National Institute of, H. I. V. V. T. N. Infectious Diseases, Phase 1 safety and immunogenicity testing of DNA and recombinant modified vaccinia Ankara vaccines expressing HIV-1 virus-like particles. J Infect Dis 203, 610–619 (2011). [PubMed: 21282192]
22. Kesavardhana S, Das R, Citron M, Datta R, Ecto L, Srilatha NS, DiStefano D, Swoyer R, Joyce JG, Dutta S, LaBranche CC, Montefiori DC, Flynn JA, Varadarajan R, Structure-based Design of Cyclically Permuted HIV-1 gp120 Trimers That Elicit Neutralizing Antibodies. The Journal of biological chemistry 292, 278–291 (2017). [PubMed: 27879316]
23. Saha P, Bhattacharyya S, Kesavardhana S, Miranda ER, Ali PS, Sharma D, Varadarajan R, Designed cyclic permutants of HIV-1 gp120: implications for envelope trimer structure and immunogen design. Biochemistry 51, 1836–1847 (2012). [PubMed: 22329717]
24. Jones AT, Chamcha V, Kesavardhana S, Shen X, Beaumont D, Das R, Wyatt LS, LaBranche CC, Stanfield-Oakley S, Ferrari G, Montefiori DC, Moss B, Tomaras GD, Varadarajan R, Amara RR, A Trimeric HIV-1 Envelope gp120 Immunogen Induces Potent and Broad Anti-V1V2 Loop Antibodies against HIV-1 in Rabbits and Rhesus Macaques. J Virol 92, (2018).
25. Jones AT, Shen X, Walter KL, LaBranche CC, Wyatt LS, Tomaras GD, Montefiori DC, Moss B, Barouch DH, Clements JD, Kozlowski PA, Varadarajan R, Amara RR, HIV-1 vaccination by needle-free oral injection induces strong mucosal immunity and protects against SHIV challenge. Nat Commun 10, 798 (2019). [PubMed: 30778066]
26. Clements JD, Norton EB, The Mucosal Vaccine Adjuvant LT(R192G/L211A) or dmLT. mSphere 3, (2018).
27. Bernstein DI, Pasetti MF, Brady R, Buskirk AD, Wahid R, Dickey M, Cohen M, Baughman H, El-Khorazaty J, Maier N, Sztein MB, Baqar S, Bourgeois AL, A Phase 1 dose escalating study of double mutant heat-labile toxin LTR192G/L211A (dmLT) from Enterotoxigenic Escherichia coli (ETEC) by sublingual or oral immunization. Vaccine 37, 602–611 (2019). [PubMed: 30563789]
28. Sahoo A, Hodge EA, LaBranche CC, Styles TM, Shen X, Cheedarla N, Shiferaw A, Ozorowski G, Lee WH, Ward AB, Tomaras GD, Montefiori DC, Irvine DJ, Lee KK, Amara RR, Structure-guided changes at the V2 apex of HIV-1 clade C trimer enhance elicitation of autologous neutralizing and broad V1V2-scaffold antibodies. Cell Rep 38, 110436 (2022). [PubMed: 35235790]
29. Yang L, Sharma SK, Cottrell C, Guenaga J, Tran K, Wilson R, Behrens AJ, Crispin M, de Val N, Wyatt RT, Structure-Guided Redesign Improves NFL HIV Env Trimer Integrity and Identifies an Inter-Protomer Disulfide Permitting Post-Expression Cleavage. Front Immunol 9, 1631 (2018). [PubMed: 30065725]
30. Bricault CA, Yusim K, Seaman MS, Yoon H, Theiler J, Giorgi EE, Wagh K, Theiler M, Hraber P, Macke JP, Kreider EF, Learn GH, Hahn BH, Scheid JF, Kovacs JM, Shields JL, Lavine CL, Ghantous F, Rist M, Bayne MG, Neubauer GH, McMahan K, Peng H, Cheneau C, Jones JJ, Zeng J, Ochsenbauer C, Nkolola JP, Stephenson KE, Chen B, Gnanakaran S, Bonsignori M, Williams LD, Haynes BF, Doria-Rose N, Mascola JR, Montefiori DC, Barouch DH, Korber B, HIV-1 Neutralizing Antibody Signatures and Application to Epitope-Targeted Vaccine Design. Cell Host Microbe 26, 296 (2019). [PubMed: 31415756]
31. Julien JP, Sok D, Khayat R, Lee JH, Doores KJ, Walker LM, Ramos A, Diwanji DC, Pejchal R, Cupo A, Katpally U, Depetris RS, Stanfield RL, McBride R, Marozsan AJ, Paulson JC, Sanders RW, Moore JP, Burton DR, Poignard P, Ward AB, Wilson IA, Broadly neutralizing antibody PGT121 allosterically modulates CD4 binding via recognition of the HIV-1 gp120 V3 base and multiple surrounding glycans. PLoS Pathog 9, e1003342 (2013). [PubMed: 23658524]
32. Zolla-Pazner S, deCamp AC, Cardozo T, Karasavvas N, Gottardo R, Williams C, Morris DE, Tomaras G, Rao M, Billings E, Berman P, Shen X, Andrews C, O'Connell RJ, Ngauy V, Nitayaphan S, de Souza M, Korber B, Koup R, Bailer RT, Mascola JR, Pinter A, Montefiori

D, Haynes BF, Robb ML, Rerks-Ngarm S, Michael NL, Gilbert PB, Kim JH, Analysis of V2 antibody responses induced in vaccinees in the ALVAC/AIDSVAX HIV-1 vaccine efficacy trial. PLoS One 8, e53629 (2013). [PubMed: 23349725]

33. Barouch DH, Liu J, Li H, Maxfield LF, Abbink P, Lynch DM, Iampietro MJ, SanMiguel A, Seaman MS, Ferrari G, Forthal DN, Ourmanov I, Hirsch VM, Carville A, Mansfield KG, Stablein D, Pau MG, Schuitemaker H, Sadoff JC, Billings EA, Rao M, Robb ML, Kim JH, Marovich MA, Goudsmit J, Michael NL, Vaccine protection against acquisition of neutralization-resistant SIV challenges in rhesus monkeys. Nature 482, 89–93 (2012). [PubMed: 22217938]
34. Roederer M, Keele BF, Schmidt SD, Mason RD, Welles HC, Fischer W, Labranche C, Foulds KE, Louder MK, Yang ZY, Todd JP, Buzby AP, Mach LV, Shen L, Seaton KE, Ward BM, Bailer RT, Gottardo R, Gu W, Ferrari G, Alam SM, Denny TN, Montefiori DC, Tomaras GD, Korber BT, Nason MC, Seder RA, Koup RA, Letvin NL, Rao SS, Nabel GJ, Mascola JR, Immunological and virological mechanisms of vaccine-mediated protection against SIV and HIV. Nature 505, 502–508 (2014). [PubMed: 24352234]
35. Burton S, Spicer LM, Charles TP, Gangadhara S, Reddy PBJ, Styles TM, Velu V, Kasturi SP, Legere T, Hunter E, Pulendran B, Amara R, Hraber P, Derdeyn CA, Clade C HIV-1 Envelope Vaccination Regimens Differ in Their Ability To Elicit Antibodies with Moderate Neutralization Breadth against Genetically Diverse Tier 2 HIV-1 Envelope Variants. J Virol 93, (2019).
36. Ackerman ME, Moldt B, Wyatt RT, Dugast AS, McAndrew E, Tsoukas S, Jost S, Berger CT, Sciaranghella G, Liu Q, Irvine DJ, Burton DR, Alter G, A robust, high-throughput assay to determine the phagocytic activity of clinical antibody samples. J Immunol Methods 366, 8–19 (2011). [PubMed: 21192942]
37. McAndrew EG, Dugast AS, Licht AF, Eusebio JR, Alter G, Ackerman ME, Determining the phagocytic activity of clinical antibody samples. J Vis Exp, e3588 (2011). [PubMed: 22143444]
38. Duerr R, Gorny MK, V2-Specific Antibodies in HIV-1 Vaccine Research and Natural Infection: Controllers or Surrogate Markers. Vaccines (Basel) 7, (2019).
39. Gudelj I, Lauc G, Pezer M, Immunoglobulin G glycosylation in aging and diseases. Cell Immunol 333, 65–79 (2018). [PubMed: 30107893]
40. Irvine EB, Alter G, Understanding the role of antibody glycosylation through the lens of severe viral and bacterial diseases. Glycobiology 30, 241–253 (2020). [PubMed: 32103252]
41. Larsen MD, de Graaf EL, Sonneveld ME, Plomp HR, Nouta J, Hoepel W, Chen HJ, Linty F, Visser R, Brinkhaus M, Sustic T, de Taeye SW, Bentlage AEH, Toivonen S, Koeleman CAM, Sainio S, Kootstra NA, Brouwer PJM, Geyer CE, Derksen NIL, Wolbink G, de Winther M, Sanders RW, van Gils MJ, de Bruin S, Vlaar APJ, Amsterdam UC, g. biobank study, Rispens T, den Dunnen J, Zaaijer HL, Wuhrer M, van der Schoot C. Ellen, Vidarsson G, Afucosylated IgG characterizes enveloped viral responses and correlates with COVID-19 severity. Science 371, (2021).
42. Ackerman ME, Das J, Pittala S, Broge T, Linde C, Suscovich TJ, Brown EP, Bradley T, Natarajan H, Lin S, Sassic JK, O'Keefe S, Mehta N, Goodman D, Sips M, Weiner JA, Tomaras GD, Haynes BF, Lauffenburger DA, Bailey-Kellogg C, Roederer M, Alter G, Route of immunization defines multiple mechanisms of vaccine-mediated protection against SIV. Nat Med 24, 1590–1598 (2018). [PubMed: 30177821]
43. Shinkawa T, Nakamura K, Yamane N, Shoji-Hosaka E, Kanda Y, Sakurada M, Uchida K, Anazawa H, Satoh M, Yamasaki M, Hanai N, Shitara K, The absence of fucose but not the presence of galactose or bisecting N-acetylglucosamine of human IgG1 complex-type oligosaccharides shows the critical role of enhancing antibody-dependent cellular cytotoxicity. J Biol Chem 278, 3466–3473 (2003). [PubMed: 12427744]
44. Scallon BJ, Tam SH, McCarthy SG, Cai AN, Raju TS, Higher levels of sialylated Fc glycans in immunoglobulin G molecules can adversely impact functionality. Mol Immunol 44, 1524–1534 (2007). [PubMed: 17045339]
45. Shields RL, Lai J, Keck R, O'Connell LY, Hong K, Meng YG, Weikert SH, Presta LG, Lack of fucose on human IgG1 N-linked oligosaccharide improves binding to human Fcgamma RIII and antibody-dependent cellular toxicity. The Journal of biological chemistry 277, 26733–26740 (2002). [PubMed: 11986321]
46. Ding J, Tasker C, Lespinasse P, Dai J, Fitzgerald-Bocarsly P, Lu W, Heller D, Chang TL, Integrin alpha4beta7 Expression Increases HIV Susceptibility in Activated Cervical CD4+ T Cells by an

HIV Attachment-Independent Mechanism. J Acquir Immune Defic Syndr 69, 509–518 (2015). [PubMed: 26167616]

47. Choe H, Chemokine receptors in HIV-1 and SIV infection. Arch Pharm Res 21, 634–639 (1998). [PubMed: 9868529]
48. Martin-Gayo E, Cronin J, Hickman T, Ouyang Z, Lindqvist M, Kolb KE, Schulze Zur Wiesch J, Cubas R, Porichis F, Shalek AK, van Lunzen J, Haddad EK, Walker BD, Kaufmann DE, Lichterfeld M, Yu XG, Circulating CXCR5(+)CXCR3(+)PD-1(lo) Tfh-like cells in HIV-1 controllers with neutralizing antibody breadth. JCI Insight 2, e89574 (2017). [PubMed: 28138558]
49. Zhang J, Liu W, Wen B, Xie T, Tang P, Hu Y, Huang L, Jin K, Zhang P, Liu Z, Niu L, Qu X, Circulating CXCR3(+) Tfh cells positively correlate with neutralizing antibody responses in HCV-infected patients. Sci Rep 9, 10090 (2019). [PubMed: 31300682]
50. Bentebibel SE, Lopez S, Obermoser G, Schmitt N, Mueller C, Harrod C, Flano E, Mejias A, Albrecht RA, Blankenship D, Xu H, Pascual V, Banchereau J, Garcia-Sastre A, Palucka AK, Ramilo O, Ueno H, Induction of ICOS+CXCR3+CXCR5+ TH cells correlates with antibody responses to influenza vaccination. Sci Transl Med 5, 176ra132 (2013).
51. Iyer SS, Gangadhara S, Victor B, Gomez R, Basu R, Hong JJ, Labranche C, Montefiori DC, Villinger F, Moss B, Amara RR, Codelivery of Envelope Protein in Alum with MVA Vaccine Induces CXCR3-Biased CXCR5+ and CXCR5- CD4 T Cell Responses in Rhesus Macaques. J Immunol 195, 994–1005 (2015). [PubMed: 26116502]
52. Geretti AM, Harrison L, Green H, Sabin C, Hill T, Fearnhill E, Pillay D, Dunn D, U. K. C. G. o. H. D. Resistance, Effect of HIV-1 subtype on virologic and immunologic response to starting highly active antiretroviral therapy. Clin Infect Dis 48, 1296–1305 (2009). [PubMed: 19331585]
53. Song RJ, Chenine AL, Rasmussen RA, Ruprecht CR, Mirshahidi S, Grisson RD, Xu W, Whitney JB, Goins LM, Ong H, Li PL, Shai-Kobiler E, Wang T, McCann CM, Zhang H, Wood C, Kankasa C, Secor WE, McClure HM, Strobert E, Else JG, Ruprecht RM, Molecularly cloned SHIV-1157ipd3N4: a highly replication- competent, mucosally transmissible R5 simian-human immunodeficiency virus encoding HIV clade C Env. J Virol 80, 8729–8738 (2006). [PubMed: 16912320]
54. Schifanella L, Barnett SW, Bissa M, Galli V, Doster MN, Vaccari M, Tomaras GD, Shen X, Phogat S, Pal R, Montefiori DC, LaBranche CC, Rao M, Trinh HV, Washington-Parks R, Liyanage NPM, Gorini G, Brown DR, Liang F, Lore K, Venzon DJ, Magnanelli W, Metrinko M, Kramer J, Breed M, Alter G, Ruprecht RM, Franchini G, ALVAC-HIV B/C candidate HIV vaccine efficacy dependent on neutralization profile of challenge virus and adjuvant dose and type. PLoS Pathog 15, e1008121 (2019). [PubMed: 31794588]
55. Petitdemange C, Kasturi SP, Kozlowski PA, Nabi R, Quarnstrom CF, Reddy PBJ, Derdeyn CA, Spicer LM, Patel P, Legere T, Kovalenkov YO, Labranche CC, Villinger F, Tomai M, Vasilakos J, Haynes B, Kang CY, Gibbs JS, Yewdell JW, Barouch D, Wrammert J, Montefiori D, Hunter E, Amara RR, Masopust D, Pulendran B, Vaccine induction of antibodies and tissue-resident CD8+ T cells enhances protection against mucosal SHIV-infection in young macaques. JCI Insight 4, (2019).
56. Malherbe DC, Vang L, Mendy J, Barnette PT, Spencer DA, Reed J, Kareko BW, Sather DN, Pandey S, Wibmer CK, Robins H, Fuller DH, Park B, Lakhashe SK, Wilson JM, Axthelm MK, Ruprecht RM, Moore PL, Sacha JB, Hessell AJ, Alexander J, Haigwood NL, Modified Adenovirus Prime-Protein Boost Clade C HIV Vaccine Strategy Results in Reduced Viral DNA in Blood and Tissues Following Tier 2 SHIV Challenge. Front Immunol 11, 626464 (2020). [PubMed: 33658998]
57. Styles TM, Gangadhara S, Reddy PBJ, Hicks S, LaBranche CC, Montefiori DC, Derdeyn CA, Kozlowski PA, Velu V, Amara RR, Human Immunodeficiency Virus C.1086 Envelope gp140 Protein Boosts following DNA/Modified Vaccinia Virus Ankara Vaccination Fail To Enhance Heterologous Anti-V1V2 Antibody Response and Protection against Clade C Simian-Human Immunodeficiency Virus Challenge. J Virol 93, (2019).
58. Om K, Paquin-Proulx D, Montero M, Peachman K, Shen X, Wieczorek L, Beck Z, Weiner JA, Kim D, Li Y, Mdluli T, Shubin Z, Bryant C, Sharma V, Tokarev A, Dawson P, White Y, Appelbe O, Klatt NR, Tovanabutra S, Estes JD, Matyas GR, Ferrari G, Alving CR, Tomaras GD, Ackerman ME, Michael NL, Robb ML, Polonis V, Rolland M, Eller MA, Rao M, Bolton

DL, Adjuvanted HIV-1 vaccine promotes antibody-dependent phagocytic responses and protects against heterologous SHIV challenge. PLoS Pathog 16, e1008764 (2020). [PubMed: 32881968]

59. Vaccari M, Gordon SN, Fourati S, Schifanella L, Liyanage NP, Cameron M, Keele BF, Shen X, Tomaras GD, Billings E, Rao M, Chung AW, Dowell KG, Bailey-Kellogg C, Brown EP, Ackerman ME, Vargas-Inchaustegui DA, Whitney S, Doster MN, Binello N, Pegu P, Montefiori DC, Foulds K, Quinn DS, Donaldson M, Liang F, Lore K, Roederer M, Koup RA, McDermott A, Ma ZM, Miller CJ, Phan TB, Forthal DN, Blackburn M, Caccuri F, Bissa M, Ferrari G, Kalyanaraman V, Ferrari MG, Thompson D, Robert-Guroff M, Ratto-Kim S, Kim JH, Michael NL, Phogat S, Barnett SW, Tartaglia J, Venzon D, Stablein DM, Alter G, Sekaly RP, Franchini G, Adjuvant-dependent innate and adaptive immune signatures of risk of SIVmac251 acquisition. Nat Med 22, 762–770 (2016). [PubMed: 27239761]
60. Alter G, Ottenhoff THM, Joosten SA, Antibody glycosylation in inflammation, disease and vaccination. Semin Immunol 39, 102–110 (2018). [PubMed: 29903548]
61. Mahan AE, Jennewein MF, Suscovich T, Dionne K, Tedesco J, Chung AW, Streeck H, Pau M, Schuitemaker H, Francis D, Fast P, Laufer D, Walker BD, Baden L, Barouch DH, Alter G, Antigen-Specific Antibody Glycosylation Is Regulated via Vaccination. PLoS Pathog 12, e1005456 (2016). [PubMed: 26982805]
62. Arunachalam PS, Charles TP, Joag V, Bollimpelli VS, Scott MKD, Wimmers F, Burton SL, Labranche CC, Petitdemange C, Gangadhara S, Styles TM, Quarnstrom CF, Walter KA, Ketas TJ, Legere T, Jagadeesh Reddy PB, Kasturi SP, Tsai A, Yeung BZ, Gupta S, Tomai M, Vasilakos J, Shaw GM, Kang CY, Moore JP, Subramaniam S, Khatri P, Montefiori D, Kozlowski PA, Derdeyn CA, Hunter E, Masopust D, Amara RR, Pulendran B, T cell-inducing vaccine durably prevents mucosal SHIV infection even with lower neutralizing antibody titers. Nat Med 26, 932–940 (2020). [PubMed: 32393800]
63. Lai L, Kwa S, Kozlowski PA, Montefiori DC, Ferrari G, Johnson WE, Hirsch V, Villinger F, Chennareddi L, Earl PL, Moss B, Amara RR, Robinson HL, in J Infect Dis (United States, 2011), vol. 204, pp. 164–173. [PubMed: 21628671]
64. Carnathan DG, Wetzel KS, Yu J, Lee ST, Johnson BA, Paiardini M, Yan J, Morrow MP, Sardesai NY, Weiner DB, Ertl HCJ, Silvestri G, Activated CD4+CCR5+ T cells in the rectum predict increased SIV acquisition in SIVGag/Tat-vaccinated rhesus macaques. Proceedings of the National Academy of Sciences 112, 518–523 (2015).
65. Vaccari M, Gordon SN, Fourati S, Schifanella L, Liyanage NPM, Cameron M, Keele BF, Shen X, Tomaras GD, Billings E, Rao M, Chung AW, Dowell KG, Bailey-Kellogg C, Brown EP, Ackerman ME, Vargas-Inchaustegui DA, Whitney S, Doster MN, Binello N, Pegu P, Montefiori DC, Foulds K, Quinn DS, Donaldson M, Liang F, Lore K, Roederer M, Koup RA, McDermott A, Ma Z-M, Miller CJ, Phan TB, Forthal DN, Blackburn M, Caccuri F, Bissa M, Ferrari G, Kalyanaraman V, Ferrari MG, Thompson D, Robert-Guroff M, Ratto-Kim S, Kim JH, Michael NL, Phogat S, Barnett SW, Tartaglia J, Venzon D, Stablein DM, Alter G, Sekaly R-P, Franchini G, Adjuvant-dependent innate and adaptive immune signatures of risk of SIVmac251 acquisition. Nat Med 22, 762–770 (2016). [PubMed: 27239761]
66. Sui Y, Dzutsev A, Venzon D, Frey B, Thovarai V, Trinchieri G, Berzofsky JA, Influence of gut microbiome on mucosal immune activation and SHIV viral transmission in naive macaques. Mucosal Immunol 11, 1219–1229 (2018). [PubMed: 29858581]
67. Harmon TM, Fisher KA, McGlynn MG, Stover J, Warren MJ, Teng Y, Naveke A, Exploring the Potential Health Impact and Cost-Effectiveness of AIDS Vaccine within a Comprehensive HIV/AIDS Response in Low- and Middle-Income Countries. PLoS One 11, e0146387 (2016). [PubMed: 26731116]
68. Havenar-Daughton C, Reiss SM, Carnathan DG, Wu JE, Kendric K, Torrents de la Pena A, Kasturi SP, Dan JM, Bothwell M, Sanders RW, Pulendran B, Silvestri G, Crotty S, Cytokine-Independent Detection of Antigen-Specific Germinal Center T Follicular Helper Cells in Immunized Nonhuman Primates Using a Live Cell Activation-Induced Marker Technique. J Immunol 197, 994–1002 (2016). [PubMed: 27335502]
69. Kulkarni V, Ruprecht RM, Mucosal IgA Responses: Damaged in Established HIV Infection-Yet, Effective Weapon against HIV Transmission. Front Immunol 8, 1581 (2017). [PubMed: 29176985]

70. Wang C, Kang SG, Lee J, Sun Z, Kim CH, The roles of CCR6 in migration of Th17 cells and regulation of effector T-cell balance in the gut. Mucosal Immunol 2, 173–183 (2009). [PubMed: 19129757]
71. Ravi AD, Sadhna D, Nagpaal D, Chawla L, Needle free injection technology: A complete insight. Int J Pharm Investig 5, 192–199 (2015).
72. Ram D, Peretz B, Administering local anaesthesia to paediatric dental patients -- current status and prospects for the future. Int J Paediatr Dent 12, 80–89 (2002). [PubMed: 11966886]
73. Hosseinipour MC, Innes C, Naidoo S, Mann P, Hutter J, Ramjee G, Sebe M, Maganga L, Herce ME, deCamp AC, Marshall K, Dintwe O, Andersen-Nissen E, Tomaras GD, Mkhize N, Morris L, Jensen R, Miner MD, Pantaleo G, Ding S, Van Der Meeren O, Barnett SW, McElrath MJ, Corey L, Kublin JG, Team HP, Phase 1 Human Immunodeficiency Virus (HIV) Vaccine Trial to Evaluate the Safety and Immunogenicity of HIV Subtype C DNA and MF59-Adjuvanted Subtype C Envelope Protein. Clin Infect Dis 72, 50–60 (2021). [PubMed: 31900486]
74. Yu C, Walter M, in Needleless Injectors for the Administration of Vaccines: A Review of Clinical Effectiveness (Ottawa (ON), 2020).
75. Gaudinski MR, Houser KV, Morabito KM, Hu Z, Yamshchikov G, Rothwell RS, Berkowitz N, Mendoza F, Saunders JG, Novik L, Hendel CS, Holman LA, Gordon IJ, Cox JH, Edupuganti S, McArthur MA, Rouphael NG, Lyke KE, Cummings GE, Sitar S, Bailer RT, Foreman BM, Burgomaster K, Pelc RS, Gordon DN, DeMaso CR, Dowd KA, Laurencot C, Schwartz RM, Mascola JR, Graham BS, Pierson TC, Ledgerwood JE, Chen GL, Vrc, V. R. C. s. teams, Safety, tolerability, and immunogenicity of two Zika virus DNA vaccine candidates in healthy adults: randomised, open-label, phase 1 clinical trials. Lancet 391, 552–562 (2018). [PubMed: 29217376]
76. Dey A, Chozhavel Rajanathan TM, Chandra H, Pericherla HPR, Kumar S, Choonia HS, Bajpai M, Singh AK, Sinha A, Saini G, Dalal P, Vandriwala S, Raheem MA, Divate RD, Navlani NL, Sharma V, Parikh A, Prasath S, Sankar Rao M, Maithal K, Immunogenic potential of DNA vaccine candidate, ZyCoV-D against SARS-CoV-2 in animal models. Vaccine, (2021).
77. Amara RR, Villinger F, Altman JD, Lydy SL, O'Neil SP, Staprans SI, Montefiori DC, Xu Y, Herndon JG, Wyatt LS, Candido MA, Kozyr NL, Earl PL, Smith JM, Ma HL, Grimm BD, Hulsey ML, McClure HM, McNicholl JM, Moss B, Robinson HL, Control of a mucosal challenge and prevention of AIDS by a multiprotein DNA/MVA vaccine. Vaccine 20, 1949–1955 (2002). [PubMed: 11983252]
78. Smoot ME, Ono K, Ruscheinski J, Wang PL, Ideker T, Cytoscape 2.8: new features for data integration and network visualization. Bioinformatics 27, 431–432 (2011). [PubMed: 21149340]
79. R: A Language and Environment for Statistical Computing (R Foundation for Statistical Computing. (https://www.R-project.org/).
80. Mahan AE, Tedesco J, Dionne K, Baruah K, Cheng HD, De Jager PL, Barouch DH, Suscovich T, Ackerman M, Crispin M, Alter G, A method for high-throughput, sensitive analysis of IgG Fc and Fab glycosylation by capillary electrophoresis. J Immunol Methods 417, 34–44 (2015). [PubMed: 25523925]
81. Hudgens MG, Gilbert PB, Assessing vaccine effects in repeated low-dose challenge experiments. Biometrics 65, 1223–1232 (2009). [PubMed: 19397589]
82. Tassaneetrithep B, Tivon D, Swetnam J, Karasavvas N, Michael NL, Kim JH, Marovich M, Cardozo T, Cryptic determinant of alpha4beta7 binding in the V2 loop of HIV-1 gp120. PLoS One 9, e108446 (2014). [PubMed: 25265384]
83. Wyatt LS, Earl PL, Liu JY, Smith JM, Montefiori DC, Robinson HL, Moss B, Multiprotein HIV type 1 clade B DNA and MVA vaccines: construction, expression, and immunogenicity in rodents of the MVA component. AIDS Res Hum Retroviruses 20, 645–653 (2004). [PubMed: 15242542]
84. Lander GC, Stagg SM, Voss NR, Cheng A, Fellmann D, Pulokas J, Yoshioka C, Irving C, Mulder A, Lau PW, Lyumkis D, Potter CS, Carragher B, Appion: an integrated, database-driven pipeline to facilitate EM image processing. J Struct Biol 166, 95–102 (2009). [PubMed: 19263523]
85. Ogura T, Iwasaki K, Sato C, Topology representing network enables highly accurate classification of protein images taken by cryo electron-microscope without masking. J Struct Biol 143, 185–200 (2003). [PubMed: 14572474]

86. Tomaras GD, Yates NL, Liu P, Qin L, Fouda GG, Chavez LL, Decamp AC, Parks RJ, Ashley VC, Lucas JT, Cohen M, Eron J, Hicks CB, Liao HX, Self SG, Landucci G, Forthal DN, Weinhold KJ, Keele BF, Hahn BH, Greenberg ML, Morris L, Karim SS, Blattner WA, Montefiori DC, Shaw GM, Perelson AS, Haynes BF, Initial B-cell responses to transmitted human immunodeficiency virus type 1: virion-binding immunoglobulin M (IgM) and IgG antibodies followed by plasma anti-gp41 antibodies with ineffective control of initial viremia. J Virol 82, 12449–12463 (2008). [PubMed: 18842730]

87. Yates NL, deCamp AC, Korber BT, Liao HX, Irene C, Pinter A, Peacock J, Harris LJ, Sawant S, Hraber P, Shen X, Rerks-Ngarm S, Pitisuttithum P, Nitayapan S, Berman PW, Robb ML, Pantaleo G, Zolla-Pazner S, Haynes BF, Alam SM, Montefiori DC, Tomaras GD, HIV-1 Envelope Glycoproteins from Diverse Clades Differentiate Antibody Responses and Durability among Vaccinees. J Virol 92, (2018).

88. Kozlowski PA, Lynch RM, Patterson RR, Cu-Uvin S, Flanigan TP, Neutra MR, Modified wick method using Weck-Cel sponges for collection of human rectal secretions and analysis of mucosal HIV antibody. J Acquir Immune Defic Syndr 24, 297–309 (2000). [PubMed: 11015145]

89. Vermont CL, van Dijken HH, van Limpt CJ, de Groot R, van Alphen L, van Den Dobbelsteen GP, Antibody avidity and immunoglobulin G isotype distribution following immunization with a monovalent meningococcal B outer membrane vesicle vaccine. Infect Immun 70, 584–590 (2002). [PubMed: 11796586]

90. Burton SL, Kilgore KM, Smith SA, Reddy S, Hunter E, Robinson HL, Silvestri G, Amara RR, Derdeyn CA, Breakthrough of SIV strain smE660 challenge in SIV strain mac239-vaccinated rhesus macaques despite potent autologous neutralizing antibody responses. Proc Natl Acad Sci U S A 112, 10780–10785 (2015). [PubMed: 26261312]

91. Charles TP, Burton SL, Arunachalam PS, Cottrell CA, Sewall LM, Bollimpelli VS, Gangadhara S, Dey AK, Ward AB, Shaw GM, Hunter E, Amara RR, Pulendran B, van Gils MJ, Derdeyn CA, The C3/465 glycan hole cluster in BG505 HIV-1 envelope is the major neutralizing target involved in preventing mucosal SHIV infection. PLoS Pathog 17, e1009257 (2021). [PubMed: 33556148]

92. Kilgore KM, Murphy MK, Burton SL, Wetzel KS, Smith SA, Xiao P, Reddy S, Francella N, Sodora DL, Silvestri G, Cole KS, Villinger F, Robinson JE, Pulendran B, Hunter E, Collman RG, Amara RR, Derdeyn CA, Characterization and Implementation of a Diverse Simian Immunodeficiency Virus SIVsm Envelope Panel in the Assessment of Neutralizing Antibody Breadth Elicited in Rhesus Macaques by Multimodal Vaccines Expressing the SIVmac239 Envelope. J Virol 89, 8130–8151 (2015). [PubMed: 26018167]

93. Alpert MD, Heyer LN, Williams DE, Harvey JD, Greenough T, Allhorn M, Evans DT, A novel assay for antibody-dependent cell-mediated cytotoxicity against HIV-1- or SIV-infected cells reveals incomplete overlap with antibodies measured by neutralization and binding assays. J Virol 86, 12039–12052 (2012). [PubMed: 22933282]

94. Karsten CB, Mehta N, Shin SA, Diefenbach TJ, Slein MD, Karpinski W, Irvine EB, Broge T, Suscovich TJ, Alter G, A versatile high-throughput assay to characterize antibody-mediated neutrophil phagocytosis. J Immunol Methods 471, 46–56 (2019). [PubMed: 31132351]

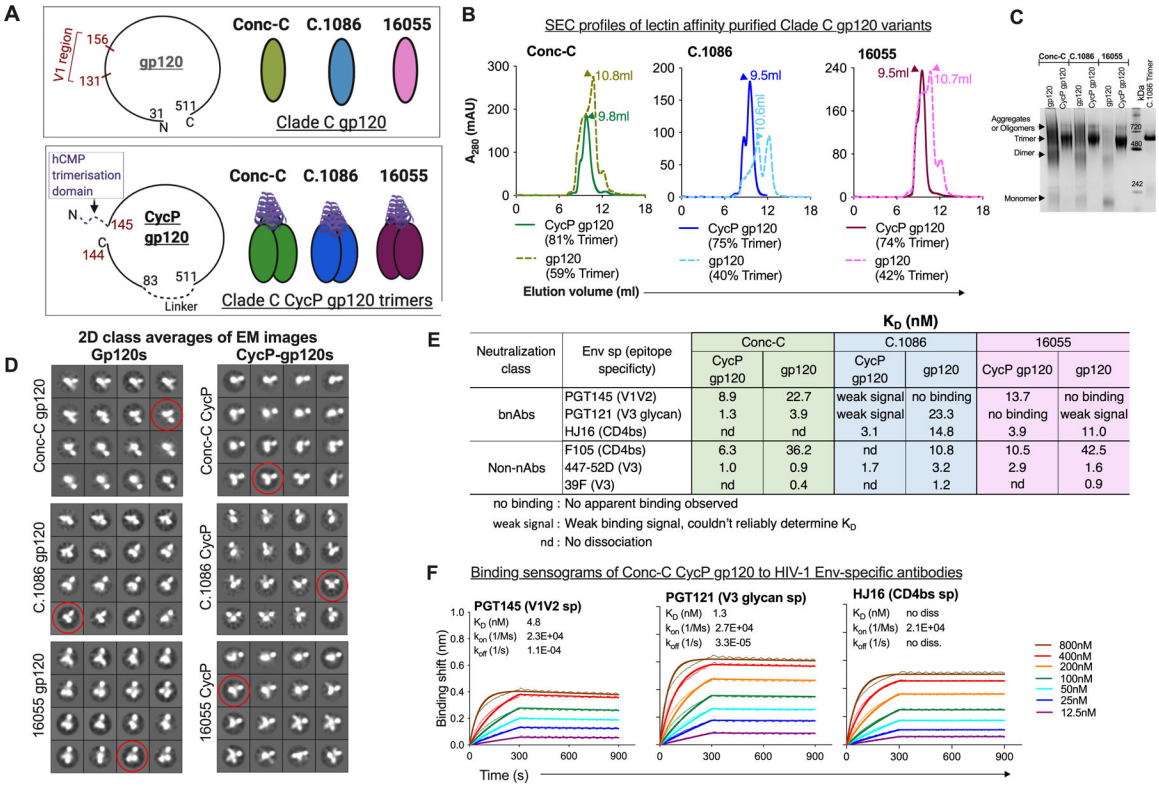

Fig. 1. Design and characterization of Clade C CycP envelope immunogens.

(A) Schematic representation of the Clade C gp120 and CycP gp120s designed in the study. (**B**) Size-exclusion chromatography (SEC) profiles of 293F expressed, *Galanthus nivalis* Lectin (GNL) affinity purified gp120 variants. Trimeric peak (arrow) elution volume (ml) indicated, trimer proportion (% AUC) for each protein mentioned below its legend. (**C**) Blue native PAGE (BN-PAGE) of purified proteins with molecular weight standard. **(D)** 2D-class averages (4×4 images) of the proteins (purified after SEC) monitored by negative stain electron-microscopy. Representative class in each dataset that resembles a trimeric particle has been circled (red). (**E**) K_D (nM) of CycP gp120 and gp120 designs against various env specific antibodies measured by Bio-layer Interferometry (BLI). Kinetic parameters calculated by globally fitting the raw data to a 1:1 binding model. Mean of K_D values calculated from more than two independent experiments indicated. (**F**) BLI binding responses of Conc-C CycP gp120 to HIV-1 env specific bnAbs. Raw traces (dotted), fit traces (solid).

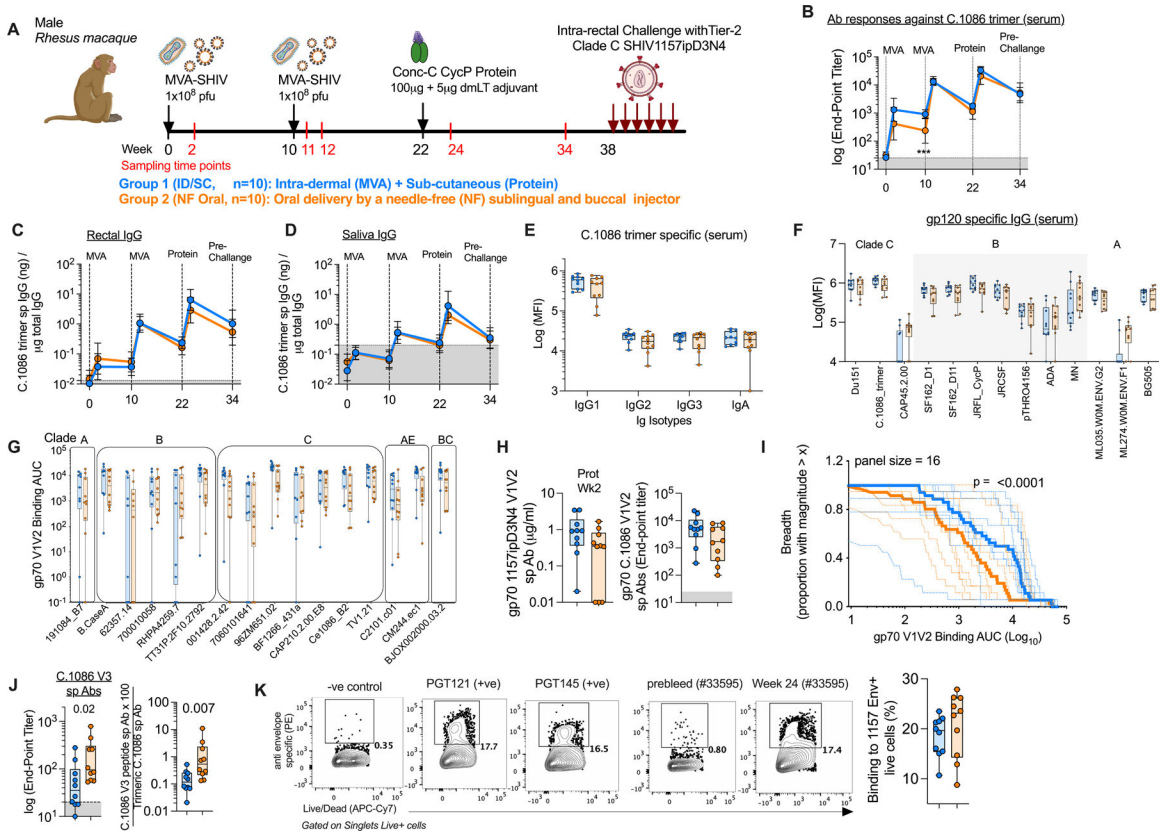

Fig. 2. Clade C MVA/CycP gp120 vaccination induces a strong antibody response in serum and rectal secretions, and broad envelope, gp70-V1V2 scaffold specific serum responses.

(**A**) Schematic overview of the MVA-SHIV/conc-C CycP gp120 vaccine efficacy study in rhesus macaques. The group color codes are followed across all panels. (**B-D**) Longitudinal antibody binding responses (geometric mean, error bars SD) in (**B**) serum, (**C**) rectal secretions, (**D**) salivary secretions measured against C.1086 trimer. (**E**) C.1086 trimer specific binding responses by IgG subclasses and IgA in serum. (**F**) Serum binding IgGs specific to a panel of diverse HIV-1 gp120 envs, including C.1086 gp140 trimer. (**G, H**) Serum antibody binding responses measured against (**G**) a panel of V1V2-scaffolds from 16 cross-clade HIV-1 isolates, and (**H left**) 1157ipD3N4 and (**H right**) C.1086 V1V2 loops scaffolded onto gp70 protein. (**I**) V1V2 Breadth magnitude curves of all immunized animals (dotted line) with median response of each group (bold line) indicated. Unpaired two-tailed Kolmogorov Smirnov test to see statistical difference between ID/SC and NF Oral groups. (**J**) Serum binding antibody responses against V3 peptide (left) and normalized to total C.1086 trimer specific responses (right). (**K**) **Left** Representative flow plots showing binding of serum collected before vaccination (pre-bleed) and two weeks after protein boost (1:100 dilution) to live transiently transfected 293T cells expressing membrane anchored 1157ipD3N4 gp160. Binding signal of vaccinated serum to MLV transfected cells was used as a negative (−ve) control to define the binding signal gate. Env specific bnAbs (PGT121, PGT145) were used as positive (+ve) controls. **Right** Frequency of 1157ipD3N4 envelope+ (Env^{+}) cells measured for each vaccinated animal. (**E-F**) Minimum-to-maximum whisker box plots with box extending from 25th to 75th percentile and line indicating

the median. (**E-K**) Serum collected two weeks after protein boost was used for analyses. (**B-D, J, H**) Shaded gray area represents background signal based on responses in pre-bleed serum. **(E, F)** Data plotted were subtracted from responses obtained from naïve rhesus macaque serum, (**G, K**) pre-bleed. All values plotted are the average of at-least two independent experiments. Statistical comparisons between groups were conducted by Mann-Whitney U test and Bonferroni correction was used to adjust for multiple comparisons. Significant findings were indicated by *p < 0.05, **p< 0.01, ***p<0.001, ****p<0.0001. ID/SC Intradermal/subcutaneous, NF Needle-free, MVA-SHIV Modified Vaccinia Ankara expressing SIV mac239 Gag/Pol and HIV-1 C.1086 gp150 Env as VLP (virus like particle). In all cases, data was monitored for n=10 animals in each vaccine arm.

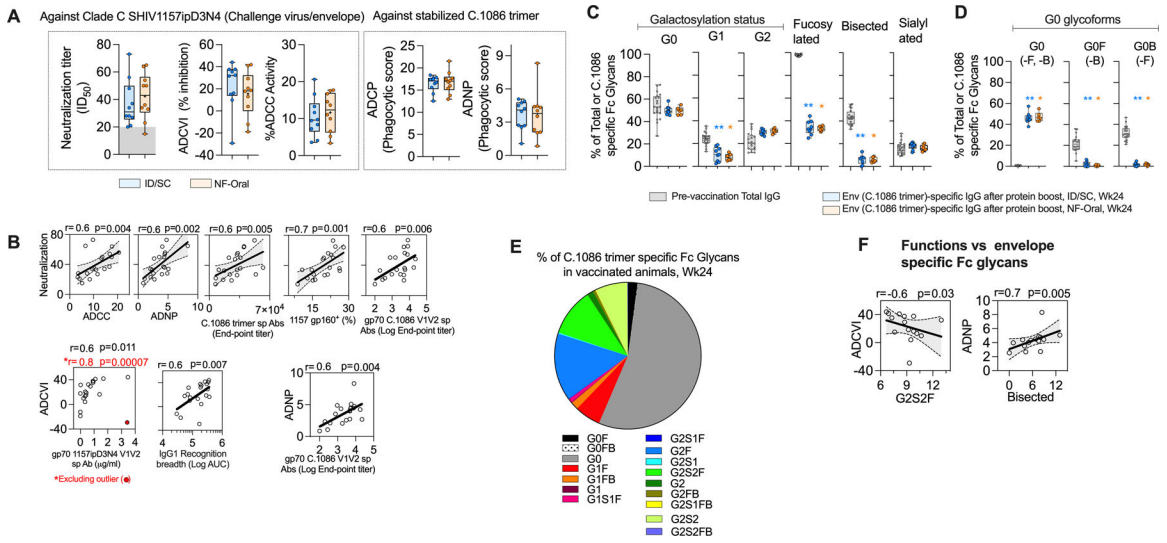

Fig. 3. Functional and biophysical characterization of serum antibody responses.

(**A**) Functional activities associated with the serum (collected two weeks after protein boost or week 24) from vaccinated animals, including neutralization, antibody-dependent cell-mediated virus inhibition (ADCVI), antibody-dependent cellular cytotoxicity (ADCC), antibody-dependent cellular phagocytosis (ADCP, monocyte mediated), antibody-dependent neutrophil phagocytosis (ADNP) activities. Neutralization was measured against SHIV 1157ipD3N4 Env G13.10 pseudotyped virus, ID50 serum dilution for 50% neutralization, titer< 20 (or background, shaded gray) shown at 15 for data representation. ADCVI and ADCC functions were measured against SHIV1157ipD3N4 (challenge virus envelope), while ADCP and ADNP activities were measured specific to C.1086 trimer. (**B**) Correlations between antigen-specific effector functions and antigen-specific antibodies in serum at Wk24. 95% confidence interval shaded gray. All significant findings are reported after adjusting for multiple comparisons by Bonferroni correction. Spearman's correlation coefficient r and two-sided p value indicated, n=20. (**C-E**) Distribution of C.1086 trimer specific IgG Fc specific (**C**) total galactosylated (G0 agalactosylated, G1 mono-galactosylated, G2 di-galactosylated), total fucosylated, total bisecting GlcNAc and total sialylated glycoforms across the immunization groups; (**D**) all G0 bearing glycoforms; (**E**) all glycoforms monitored in the study (G0 agalactosylated, G1 mono-galactosylated, G2 di-galactosylated, F fucosylated, B bisecting GlcNAc, S1 mono-sialylated, S2 di-sialylated, nomenclature as described by Mahan et al., 2015 (80), responses from both groups (n=15) shown due to similar distribution profile of the glycoforms across the vaccination groups, see fig. S4D). In (**C, D**), total IgG Fc glycoform of pre-vaccination serum has also been shown in gray to indicate its baseline level, n=20. Wilcoxon matched-pairs signed rank two-tailed test for statistical comparison between two time-points within vaccinated groups i.e. Fc glycoform specific to total IgG sampled pre-vaccination and Fc glycoform related to Env-specific IgG sampled after protein boost, Wk24. Bonferroni correction used to adjust for multiple comparisons, significant findings were indicated by *p < 0.05, **p< 0.01, ***p<0.001, ****p<0.0001. p values group wise color coded and indicated above group specific data show comparison relative to group specific pre-vaccination data. (**F**) Relationship between different effector functions and Env-specific Fc glycoforms. 95%

confidence interval shaded gray. Spearman's correlation coefficient r and two-sided p value indicated, n=15. (**C-F**) All plots corresponding to Env-specific Fc glycoforms contain data from 15 vaccinated animals, serum collected at Wk24. Data was not available for 5 animals due to low concentration of Env-specific IgG in the serum samples. (**A, C, D**) All Responses measured in ID/SC group are colored blue, and NF-Oral group colored orange in all panels. Box and whiskers plots where box extend from 25th to 75th percentile, median indicated by line, minimum and maximum values indicated by whiskers. All values plotted are the average of at-least two independent experiments. ID/SC Intradermal/subcutaneous, NF-Oral Needle-free Oral vaccine groups. In all cases, data was monitored for n=10 animals in each vaccine arm, unless otherwise indicated.

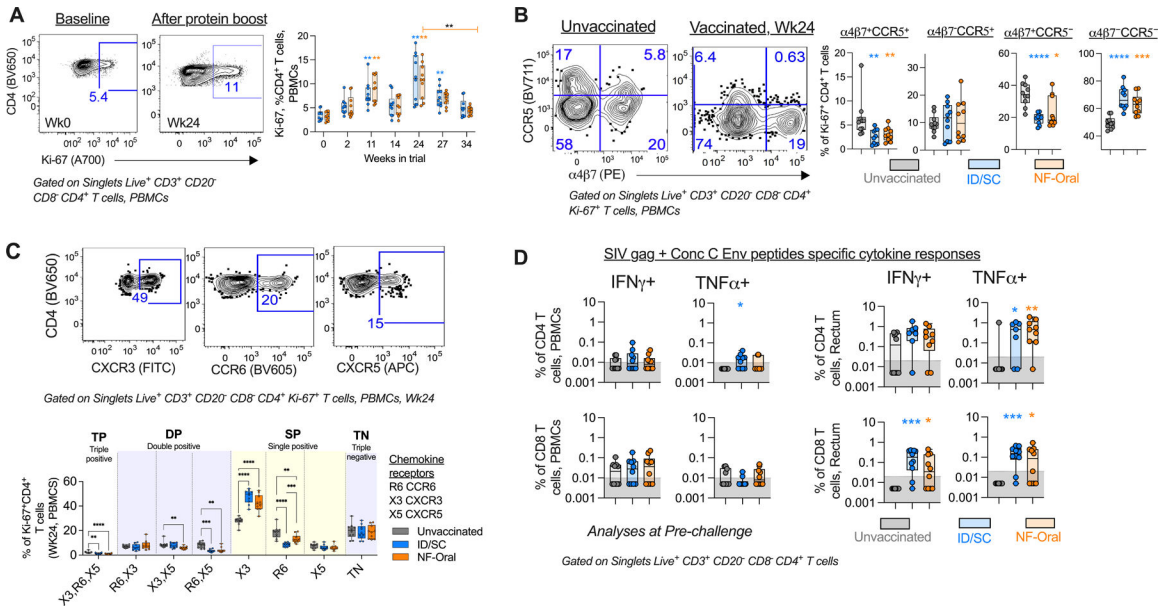

Fig. 4. Characterization of T cell responses after vaccination.

(A) Right, Temporal profile of circulating Ki-67$^+$ CD4$^+$ T cells (geomean in solid lines); **Left**, representative flow cytometry staining for a vaccinated animal. Wilcoxon matched-pairs signed rank test, two-tailed for statistical comparison within vaccinated groups. (**B**) **Right**, Scatter plot showing altered distribution of the fraction of circulating Ki-67$^+$CD4$^+$ T cells expressing α4β7/CCR5 chemokine receptors; important for permitting HIV-1 pathogenesis, at the peak proliferation phase of cells after vaccination (wk24) relative to unvaccinated control; **Left**, Representative flow staining. (**C**) **Top**, Representative flow staining showing gates used to monitor the co-expression of chemokine receptors on Ki-67$^+$ CD4$^+$ T cells and **Bottom** their comparative analyses using a Boolean function in FlowJo v9.9.6. One way ANOVA for statistical comparisons followed by Mann-Whitney U test for statistical comparison between groups. (**D**) Vaccine specific (SIV gag + Consensus C Env peptide pool) cytokine responses measured for CD4$^+$ and CD8$^+$ T cells present in blood and rectal tissue at pre-challenge (Wk34 or 4 weeks prior to intra-rectal SHIV challenge), n=10 in each vaccine arm and n=10 unvaccinated animals. For cytokine responses measured for rectal CD4$^+$ T cells, n=7 ID/SC and n=9 NF-Oral due to data not available for animals with low CD4 T cell counts (<1000, threshold). Cells stimulated with PMA/Ionomycin and blank (non-stimulated) served as positive and negative controls respectively to define gates. Mann-Whitney U test for all statistical comparison between groups. All statistical analyses have been corrected for multiple comparisons using Bonferroni correction, except TNFα$^+$ rectal CD4 T cell responses for ID/SC vs unvaccinated comparison. All comparisons found to be significant after correcting for multiple testing are indicated by *p < 0.05, **p< 0.01, ***p<0.001, ****p<0.0001. All Responses measured for ID/SC group indicated in blue, and NF-Oral group in orange. Box and whiskers plots where box extend from 25th to 75th percentile, median indicated by line, minimum and maximum values indicated by whiskers. (**A**) p values group wise color coded and indicated above group specific data indicate comparison relative to group specific pre-bleed response, or (**B-D**) responses measured relative to unvaccinated control animals, unless otherwise indicated. ID/SC Intradermal/

subcutaneous, NF-Oral Needle-free Oral vaccine groups. In all cases, data was monitored for n=10 animals in each vaccine arm and n=10 unvaccinated animals, unless otherwise indicated.

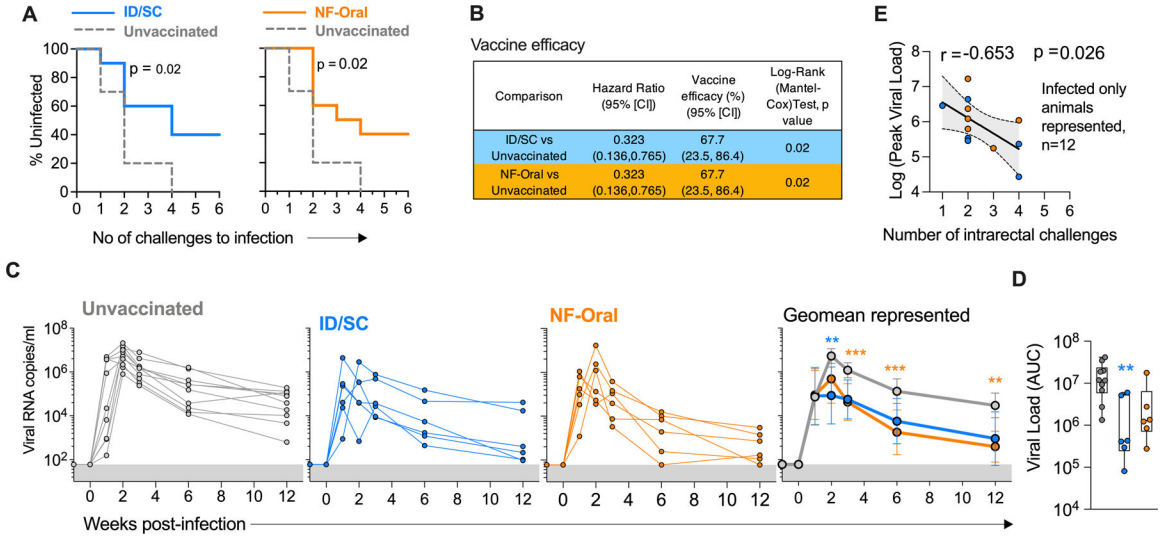

Fig. 5. MVA-HIV/cycP-gp120 vaccination protects rhesus macaques from mucosal Clade C SHIV challenge and controls viral replication irrespective of the immunization route.

(A) Acquisition of SHIV infection in ID/SC (n=10), NF-Oral (n=10) vaccinated and unvaccinated (n=10) animals (Kaplan-Meier curves and Log-rank (Mantel-Cox) test), intra-rectally challenged with tier2 pathogenic Clade C SHIV1157ipD3N4. **(B)** Vaccine efficacy of the two vaccinated groups vs control animals calculated as described previously (81). (**C**) Kinetics of plasma viral loads in unvaccinated (n=10, infected), vaccinated ID/SC (n=6, infected) and NF-Oral (n=6, infected) animals. Geomean ± 95%CI shown in the right-most graph. (**D**) Vaccination results in reduction in viral load (measured as AUC) relative to unvaccinated controls. Box and whiskers plots where box extend from 25th to 75th percentile, median indicated by line, minimum and maximum values indicated by whiskers. (**C, D**) Mann-Whitney U test for statistical comparison between groups followed by Bonferroni correction for multiple comparisons; significant p values after correcting for multiple comparisons indicated by *p < 0.05, **p< 0.01, ***p<0.001, ****p<0.0001. p values group color coded indicate comparison relative to controls. (**E**) Peak viral load monitored after infection inversely correlated with number of challenges for infection for all vaccinated infected animals (n=12), 95% confidence band shaded gray. Spearman's correlation coefficient r and two-sided p-value indicated. ID/SC Intradermal/subcutaneous, NF-Oral Needle-free Oral vaccine groups.

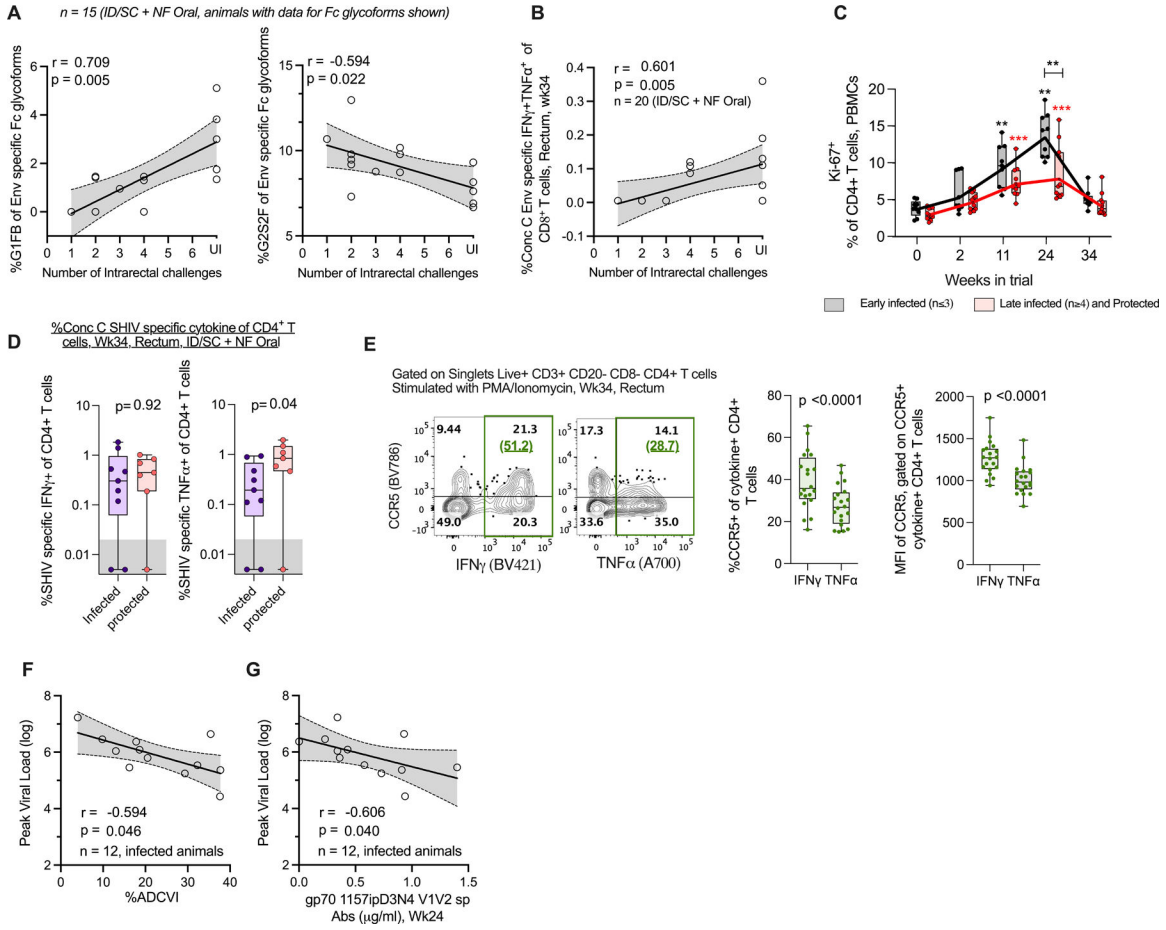

Fig. 6. Vaccine specific humoral and T cell responses are associated with protection and reduced viral replication after mucosal SHIV challenge

(A) C.1086 trimer Env-specific IgG Fc glycoforms G1FB and G2S2F correlate with reduced and enhanced risk of SHIV infection, respectively. The plots contain data from n=15 vaccinated animals. Data was not available for 5 animals due to low concentration of Env-specific IgG in the serum samples. UI Uninfected. (**B**) Consensus C Env-specific IFNγ^{+}TNFα^{+} CD8^{+} T cell responses measured at pre-challenge in rectum for all vaccinated animals (n=20, some data points overlap in the plot) associate with reduced risk of infection. UI Uninfected. (**C**) Kinetics of circulating Ki-67^{+} CD4^{+} T cells for vaccinated animals stratified into early infection acquirers (≤3 challenges, n=9) and late acquirers or protected (≥4 challenges or completely protected, n=11). Solid lines indicate geo-mean. Prior to vaccination or wk0, Peak effector response after MVA-1, MVA-2, protein boost i.e. WK2, Wk11 and Wk24, respectively, Pre-challenge wk34 or 4 weeks before virus exposure. Wilcoxon matched-pairs signed rank two-tailed test for statistical comparison within the groups, and Mann-Whitney U test for comparisons between groups. Comparisons found significant after correcting for multiple testing by Bonferroni correction indicated by *p < 0.05, **p< 0.01, ***p<0.001, ****p<0.0001. p values group wise color coded and indicated above group specific data indicate comparison relative to group specific pre-vaccination response, or otherwise indicated. (**D**) Protected vaccinated animals have (**left**) similar levels of Consensus C SHIV-specific IFNγ^{+}, and (**right**) higher levels of

TNFα$^+$ CD4$^+$ T cell responses at pre-challenge in rectum relative to infected vaccinees, Data for animals with rectal CD4 T cell counts > 1000 (threshold) shown, n=9 infected, n= 7 protected,. Unpaired two-tailed t-test for statistical comparison between groups. (**E**) CD4$^+$ T cells in rectum producing TNFα after *in-vitro* stimulation with PMA/Ionomycin express significantly lower CCR5 (both as (**middle**) fraction and (**right**) mean fluorescence intensity per cell, MFI) relative to IFNγ$^+$ producing CD4$^+$ T cells, n=20 vaccinated animals. Wilcoxon matched-pairs signed rank test, two-tailed for statistical comparison between groups. Representative plot shown in left with %CCR5$^+$ of cytokine$^+$ CD4$^+$ T cells indicated in green parenthesis. (**F,G**) Correlation between peak viral load and challenge virus-specific (**F**) ADCVI activity, (**G**) gp70 V1V2-antibodies for all infected vaccinated animals, n=12. In (**A, B, F**) Spearman's correlation coefficient r and two-sided p-value indicated, 95% confidence band shaded gray. In (**C-E**) Box and whiskers plots where box extend from 25th to 75th percentile, median indicated by line, minimum and maximum values indicated by whiskers. P values reported in **A, B, F, G** are not adjusted for multiple comparisons. The un-adjusted and adjusted p-values for the immune parameters used to report correlations with protection and peak viral load are shown in table S3. ID/SC Intradermal/subcutaneous, NF-Oral Needle-free Oral vaccine groups.